IMM 407
January 1975

Courant Institute of
Mathematical Sciences

Final Report, I

J. J. Stoker and E. Isaacson

Sponsored by Advanced Research Projects Agency,
ARPA Order No. 2774.

New York University

ARPA Order No.: 2774

IMM 407
January 1975

New York University

Courant Institute of Mathematical Sciences

FINAL REPORT, I

J. J. Stoker and E. Isaacson

This research was supported by the Advanced Research Projects Agency of the Department of Defense and was monitored under Grant DA-ARO-D-31-124-72-G113 for the period Feb. 15, 1972 - May 31, 1973 and Grant DA-ARO-D-31-124-73-G150 for the period June 1, 1973 - May 31, 1974. This work continues under Grant AFOSR-74-2728 for the period June 1, 1974 - Jan. 31, 1975.

Table of Contents

Foreword

The Courant Institute of Mathematical Sciences began a major research program in climatology under ARPA sponsorship through Grant DA-ARO-D-31-124-72-G113 for the period Feb. 15, 1972 - May 31, 1973 and the work continued under Grant DA-ARO-D-31-124-73-G150 for the period June 1, 1973 - May 31, 1974. The principal objectives were to:

a) determine the reliability of climatic predictions that result from the long-term numerical solution of general atmospheric circulation models (GCM),

b) devise more efficient numerical methods for solving the initial value problem for partial differential equations that are defined over a rotating sphere,

c) develop a theoretical basis for analyzing the behavior of solutions, for large time, of systems of equations of a type that model atmospheric flows, and

d) examine the solutions of zonally averaged atmospheric models.

The achievements of the research team are described in the final report on the above grants, by its two principal investigators, Prof. J. J. Stoker and Prof. Eugene Isaacson.

The ARPA sponsorship continues under Grant AFOSR-74-2728 to extend the above program.

P. D. Lax
Director

1. Introduction

The work in climatology at the Courant Institute of Mathematical Sciences of New York University (CIMS-NYU) began in February 1972 under ARPA sponsorship. This is a final report on the activities credited to Grant DA-ARO-D-31-124-72-G113 for the period Feb. 15, 1972 - May 31, 1973 and to Grant DA-ARO-D-31-124-73-G150 for the period June 1, 1973 - May 31, 1974.

Of primary interest is the determination of the reliability and efficiency of schemes for numerical integration over a long time period, of a system of partial differential equations for fluid motion on a sphere. That is, the work is intended to contribute to the understanding of the climatological significance of a long term numerical integration of an atmospheric global circulation model (GCM) such as that of Mintz-Arakawa [7 ;10; 4].* The simplest mathematical system for fluid flow over a sphere is that of a one layer incompressible model. In Section 2, the equations are presented. They have been extensively used to study the efficiency and accuracy of numerical integration methods for forecasting purposes [3 ;5 ;6 ;13]. The unknown variables are essentially the height, h, of the layer and the two tangential velocity components, u and v. A tangential friction force, proportional to the square of the velocity, is introduced into the two velocity equations, in order to represent the dissipation as in the Mintz-Arakawa model (see [4]).

---

* Admittedly, a GCM would have to treat the oceanic circulation, if the model were to be used for truly long period numerical studies. The GCM's of Mintz-Arakawa, of NCAR, of NOAA, and of NASA-GISS do not at present incorporate a model for the oceanic circulation.

In order to simulate the climate, it was proposed to consider a flow that could be described approximately as follows: There is a low pressure center at each pole and three "semi-permanent" high pressure cells in each hemisphere, uniformly and symmetrically placed at about $\pm 30^\circ$ latitude. Denote this basic climatological flow by $(u_c, v_c, h_c) \equiv W_c$. The differential equations for $W \equiv (u,v,h)$ are represented by

$$(1.1) \qquad L(W) = L(W_c) ,$$

with $W(0) = W_c(0)$ as the initial conditions.

Hence, a solution is given by $W = W_c$. But, the primary objective of this work is to investigate the numerical solution of (1.1); that is, to find the solution W_Δ of a finite difference approximation of (1.1):

$$(1.2) \qquad L_\Delta(W_\Delta) = L(W_c) , \quad W_\Delta(0) = W_c(0) .$$

In (1.2), L_Δ represents a discrete approximation of the differential operator L.

Three different numerical methods (i.e., L_Δ) have been programmed for the approximate solution of the system of equations (1.1). The friction coefficient is chosen so that the "spin-down" time of the homogeneous form of system (1.2) is about 10 days. The schemes are described in Sections 3, 4 and 5.

In order to represent the basic climatological flow, W_c, a study was made of the motion of vortices in a planar, one layer model. H. J. Stewart's work [11] on the stability of certain planar

vortex " solutions" was extended by G. Morikawa and E. Swenson [9; 8]. That is, Stewart used three anti-cyclonic vortices situated on a circle of radius r, to model the three semi-permanent, sub-tropical highs of the northern hemisphere, while Morikawa and Swenson, in addition, introduced a cyclonic vortex at the center of the circle to simulate the effect of the polar low. In preparation is a report by L. Bauer and G. Morikawa on the choice of parameters that yield climatologically realistic motions of the vortices, along with a study of the stability of the system for the complete range of parameters. The vortex approximation of the stationary highs and the polar lows is singular. The mathematical singularities are removed smoothly to generate the basic flow, W_c. A brief account of this vortex work leading to the definition of W_c is given in Section 2.

In order to provide a more realistic approximation for the basic spherical flow, the study of spherical vortex flows was begun by S. Friedlander and A. S. Peters. S. Drew analyzed the general circulation pattern that results from a zonally averaged model. M. Ghil completed a preliminary study of the initialization problem. A listing is given in Section 6 of all of the papers and reports credited to this program, along with a brief account of the ongoing work that has not yet been published.

In Final Report, II for the ARPA Grant AFOSR-74-2728, extensions of this climatology activity will be described.

2. The Mathematical Model, Coefficient of Friction, Zonal Flow, Basic Climatological Flow

The two-dimensional flow of an inviscid, incompressible fluid layer, for which the hydrostatic approximation is made and which is subject to friction as it moves over a perfectly spherical earth of radius a, is governed by two equations for the tangential components of velocity, u and v:

$$(2.1) \qquad \frac{D}{Dt} u - (f + \frac{u}{a} \tan \theta)v + \frac{g}{a \cos \theta} \frac{\partial h}{\partial \lambda} + Ruq = 0 ,$$

$$(2.2) \qquad \frac{D}{Dt} v + (f + \frac{u}{a} \tan \theta)u + \frac{g}{a} \frac{\partial h}{\partial \theta} + Rvq = 0 ,$$

where

$$\frac{D}{Dt} \equiv \frac{\partial}{\partial t} + \frac{u}{a \cos \theta} \frac{\partial}{\partial \lambda} + \frac{v}{a} \frac{\partial}{\partial \theta} ;$$

and the equation of continuity for the free surface height of the layer, h:

$$(2.3) \qquad \frac{\partial h}{\partial t} + \frac{1}{a \cos \theta} [\frac{\partial}{\partial \lambda} (hu) + \frac{\partial}{\partial \theta} (hv \cos \theta)] = 0 ;$$

the system (2.1)-(2.3) can be represented as the homogeneous system

$$L(W) = 0 ,$$

where W is a vector with three components, (u,v,h). The independent variables λ and θ represent longitude and latitude respectively, with corresponding components of velocity, u and v; g is the gravitational constant; $f \equiv 2\Omega \sin \theta$ is the Coriolis parameter, where Ω

is the rate of angular rotation of the earth; while R is a constant coefficient so that the friction force is thus taken proportional to the square of the velocity, since $q \equiv \sqrt{u^2 + v^2}$ represents the speed of the flow.

In a series of papers [3 ;5 ;6 ;13] the equations (2.1)-(2.3) are used with R = 0. The quadratic friction term appears in the Mintz-Arakawa equations for the motion of the atmospheric layer that is next to the surface of the earth (see [4]). A value for R is found by requiring that the "spin-down" time of the system (2.1)-(2.3) be about 10 days.* That is, the variable $W \equiv (u,v,h)$ is chosen at time t = 0 to represent a steady, purely zonal flow (see (2.5)) with maximum velocity, Q; while for the homogeneous difference equations that approximate the system (2.1)-(2.3),

$$L_{\Delta}(W_{\Delta}) = 0 ,$$

a value of R is found so that the maximum speed of the solution, $W_{\Delta}(t)$, at t = 10 days, is reduced to .1Q.

The order of magnitude of R can be determined by considering the decay of the solution, u, of

---

* This value of the spin-down time was suggested by L, Gates, A. Kasahara, C. Leith, R. Somerville, W. Washington and others in July 1973, at an informal climatology meeting at the National Center for Atmospheric Research. Numerical experiments on global circulation models indicate that for an atmosphere which is initially at rest, about three weeks are required for the normal flow patterns to develop as a result of the action of the sun, etc. This interval of time is called spin-up time. It is natural to call spin-down time, the time required for the normal flow pattern to dissipate, in the total absence of external energy sources.

$$\frac{du}{dt} = -Ru^2 , \tag{2.4}$$
$$u(0) = Q .$$

For $Q = 5$ meters/second, the value $R \cong .2(10^{-5}) \frac{1}{\text{meter}}$ yields $u(T) = .1Q$, for $T = 10$ days. In fact, since

$$u(T) = \frac{Q}{1 + RQT} ,$$

$RQT = 9$ is the formula for determining R so that $u(T) = .1Q$.

For the frictionless system (2.1)-(2.3), i.e. $R = 0$, a steady zonal solution is given by:

$$u = Q \cos \theta ,$$
$$v = 0 , \tag{2.5}$$
$$h = D - \frac{1}{g} \left(a\Omega Q + \frac{Q^2}{2}\right)\sin^2\theta .$$

The steady flow (2.5) was used to test the difference scheme that is based on stereographic coordinates (see Section 3). The fact that the equations (2.5) do not depend on the longitude, makes the zonal solution unsuitable for fully testing finite difference schemes based on "natural" spherical coordinates. Hence, for tests of numerical methods, it is convenient to consider the flow equations that result from an "unnatural" spherical coordinate system, that is, one fixed in the rotating "earth", but for which the axis of the coordinate system is perpendicular to the axis of rotation of the earth (see [12;13]). The new velocity variables, (u,v),

satisfy the system (2.1)-(2.3) in the new independent variables, (λ, θ), provided that the new Coriolis parameter, $\tilde{f}$, defined by

$$\tilde{f} = 2\Omega \cos \lambda \cos \theta \,, \tag{2.6}$$

replaces f in (2.1) and (2.2). In this case, the original steady zonal flow, about the axis of rotation of the earth, is given by:

$$\begin{aligned} u &= -Q \cos \lambda \sin \theta \,, \\ v &= Q \sin \lambda \,, \\ h &= D - \frac{1}{g}\left(a\Omega Q + \frac{Q^2}{2}\right)\cos^2\lambda \cos^2\theta \,. \end{aligned} \tag{2.7}$$

The steady flow (2.7) was used to test the two difference schemes that are based on spherical coordinates (see Sections 4 and 5).

The basic climatological flow, W_c, is defined by using the geostrophic planar vortex flows, W_p, studied by L. Bauer and G. Morikawa [2]. That is, for a rectangular coordinate system (x,y) on a tangent plane that is rigidly attached at the north pole, $(0,0)$, the rectangular velocity components, (u_p, v_p), and height, h_p, of the flow, W_p, are given by

$$u_p = -\Psi_y \,, \tag{2.8}$$

$$v_p = \Psi_x \,, \tag{2.9}$$

$$h_p = D + \frac{f}{g}\Psi \,, \tag{2.10}$$

where, with $\kappa = \dfrac{2\Omega}{\sqrt{gD}}$,

$$(2.11) \qquad \Psi = -\frac{1}{2\pi}\sum_{i=0}^{3} \gamma_i K_o(\kappa\rho_i) \ .$$

Here, the variables (u_p, v_p, h_p) and the stream function Ψ, are functions of position, (x,y), and time, t, by virtue of the definition,

$$(2.12) \qquad \rho_i^2 \equiv [x-x_i(t)]^2 + [y-y_i(t)]^2$$

where $(x_o(t), y_o(t))$ is the "center" of the polar low, while $(x_i(t), y_i(t))$ for $i = 1,2,3$ are the "centers" of the semi-permanent, sub-tropical highs. The constant $\gamma_o \geq 0$ determines the strength of the polar vortex while the constants $\gamma_1 = \gamma_2 = \gamma_3 = -\gamma < 0$, determine the strengths of the vortices that generate the highs. The distances $\sqrt{x_i^2 + y_i^2}$, are approximately the spherical distance between the pole and the sub-tropical highs on the earth. The modified Bessel function of the second kind and order 0, $K_o(x)$, has the properties:

$$(2.13) \qquad \begin{aligned} &K_o(x) + \log x \to 0 \quad &&\text{as} \quad x \to 0 \ , \\ &K_o(x) \sim \sqrt{\frac{\pi}{2x}}\, e^{-x} \quad &&\text{as} \quad x \to \infty \ . \end{aligned}$$

The derivative of $K_o(x)$ satisfies:

$$(2.14) \qquad K_o'(x) = -K_1(x) \ ,$$

where $K_1(x)$ is the modified Bessel function of order 1, for which:

$$K_1(x) - \frac{1}{x} \to 0 \qquad \text{as} \qquad x \to 0 \, ,$$

$$(2.15) \qquad K_1(x) \sim \sqrt{\frac{\pi}{2x}}\, e^{-x} \qquad \text{as} \qquad x \to \infty \, ,$$

$$K_1'(x) = -K_0(x) - \frac{1}{x} K_1(x) \, .$$

The centers of the vortices satisfy a system of eight first order ordinary differential equations, analogous to the equations for the motion of the logarithmic vortices occurring in two dimensional, incompressible fluid flows (see [2]). The condition that the vortices are in stationary equilibrium, with the three highs uniformly spaced on a circle of radius r, about the polar vortex, is that

$$(2.16) \qquad \frac{\gamma_0}{\gamma} = \sqrt{3}\, \frac{K_1(\kappa r\sqrt{3}\,)}{K_1(\kappa r)} \, .$$

Under small perturbation, the system of vortices satisfies approximately a linearized system of ordinary differential equations with constant coefficients. The perturbed motions have several natural periods of oscillation that depend on the value of κr. In fact, Bauer and Morikawa find that for

$$\kappa r = 3.75 \, ,$$

the system has a short period of about 1 year and a long period of about 12 years. Note that for $\kappa r = 3.75$,*

* For $\kappa r = 3.5$, the ratio $\gamma_0/\gamma = .0978...$ provides a state of stationary equilibrium; with a short period of about .8 year and a long period of about 8 years.

$$(2.16') \qquad \frac{\gamma_o}{\gamma} = .0816\ldots \; .$$

As indicated by Stewart [11], in his earlier study that did not include the polar low, a mean sea-level pressure of $1.013 \times 10^6 \frac{\text{dynes}}{\text{cm}^2}$ and a constant density of $1.22 \times 10^{-3} \frac{\text{gm}}{\text{cm}^3}$, correspond to a hydrostatic height, $D \cong 8.5\text{km}$ and gravity wave speed, $\sqrt{gD} \cong 2.87 \times 10^4 \frac{\text{cm}}{\text{sec}}$. Hence for the polar tangent plane, rotating at the angular velocity, Ω,

$$\frac{1}{\kappa} = \frac{\sqrt{gD}}{2\Omega} \cong 1.97 \times 10^3\text{km} \; .$$

Therefore

$$(2.17) \qquad r = r_p \equiv \frac{3.75}{\kappa} \cong 7.4 \times 10^3\text{km} \; ,$$

represents the spherical distance, r_p, of the sub-tropical latitude circle, from the north pole. That is, the sub-tropical highs are approximately at 23.5° N latitude, in this representation.

Of course, the vortex approximation for the polar cyclone and sub-tropical anti-cyclones is singular. That is, from equations (2.10)-(2.13) it follows that

$$|h_p| \to \infty \quad \text{as} \quad (x,y) \to (x_i, y_i) \; ;$$

furthermore, the planar approximation uses a constant Coriolis parameter, f. Therefore, it is a fact of great interest that the value of r_p (with a reasonable choice of D) corresponds to the latitude of the sub-tropical highs as a result of requiring the vortices to have the yearly period of the earth's revolution about the sun! However, in order to construct W_c it is necessary to eliminate the

logarithmic singularities and to "map" the flows onto the sphere. Elimination of the singularities is carried out first for the planar flow. That is, a planar, basic climatological flow, denoted by W_{cp}, is given by equations (2.8)-(2.11) with the function K_o replaced by the function $\hat{K}_o$, defined as follows:

Let

$$g(x) \equiv \sqrt{\frac{\pi}{2x}}\, e^{-x} ,$$

(2.18)
$$\hat{K}_o(x) \equiv \begin{cases} P_7(x) , & 0 \leq x \leq x_1 , \\ g(x) , & x_1 \leq x , \end{cases}$$

where x_1 is some suitably chosen value, $P_7(x)$ is a polynomial of degree seven, and $g(x)$ is the first term in the asymptotic expansion of $K_o(x)$. Here, $P_7(x)$ is defined by requiring:

(2.19)
$$P_7(0) = b, \quad P_7'(0) = P_7''(0) = P_7'''(0) = 0 ,$$
$$P_7(x_1) = g(x_1), \quad P_7'(x_1) = g'(x_1), \quad P_7''(x_1) = g''(x_1), \quad P_7'''(x_1) = g'''(x_1),$$

where b is found by linear extrapolation of $g(x)$, from $x = x_1$, i.e.

(2.20)
$$b = g(x_1) - x_1 g'(x_1) .$$

In figure 1, graphs of $\hat{K}_o(x)$ are drawn for $x_1 = 1.762$, 2.013, and 2.265. Plots of $\hat{K}_1(x)$, defined by

(2.21)
$$\hat{K}_1(x) = -\hat{K}_o'(x) ,$$

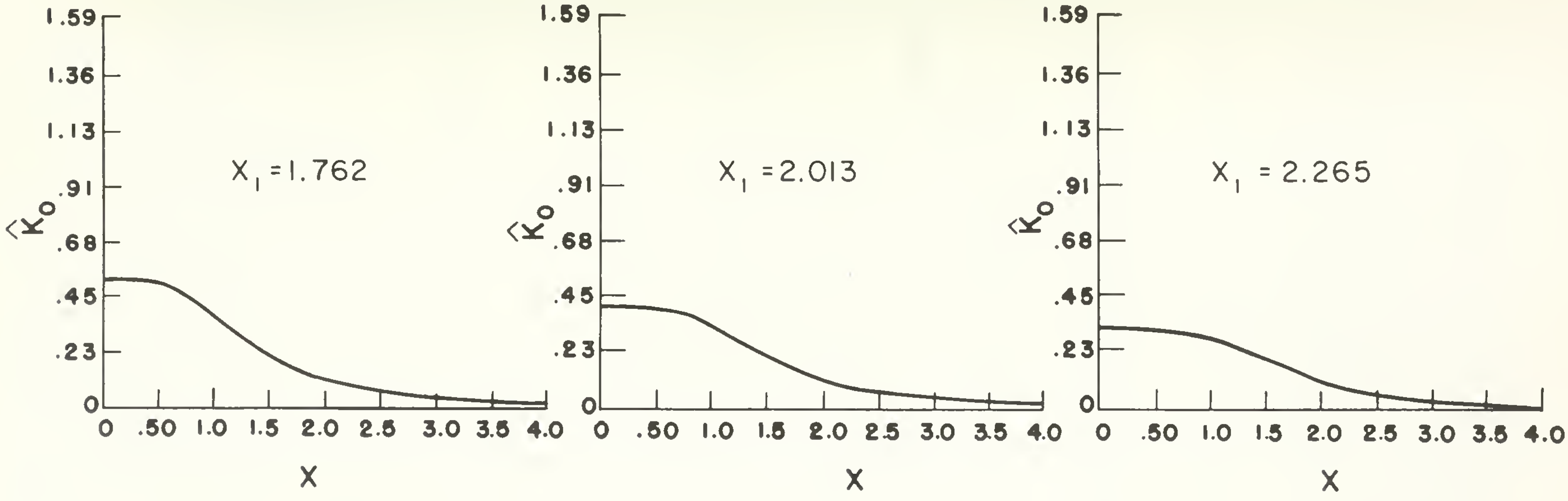
$\hat{K}_0$
$X_1 = 1.762$
$X_1 = 2.013$
$X_1 = 2.265$
X
1.59
1.36
1.13
.91
.68
.45
.23
0
0 .50 1.0 1.5 2.0 2.5 3.0 3.5 4.0

FIG. I

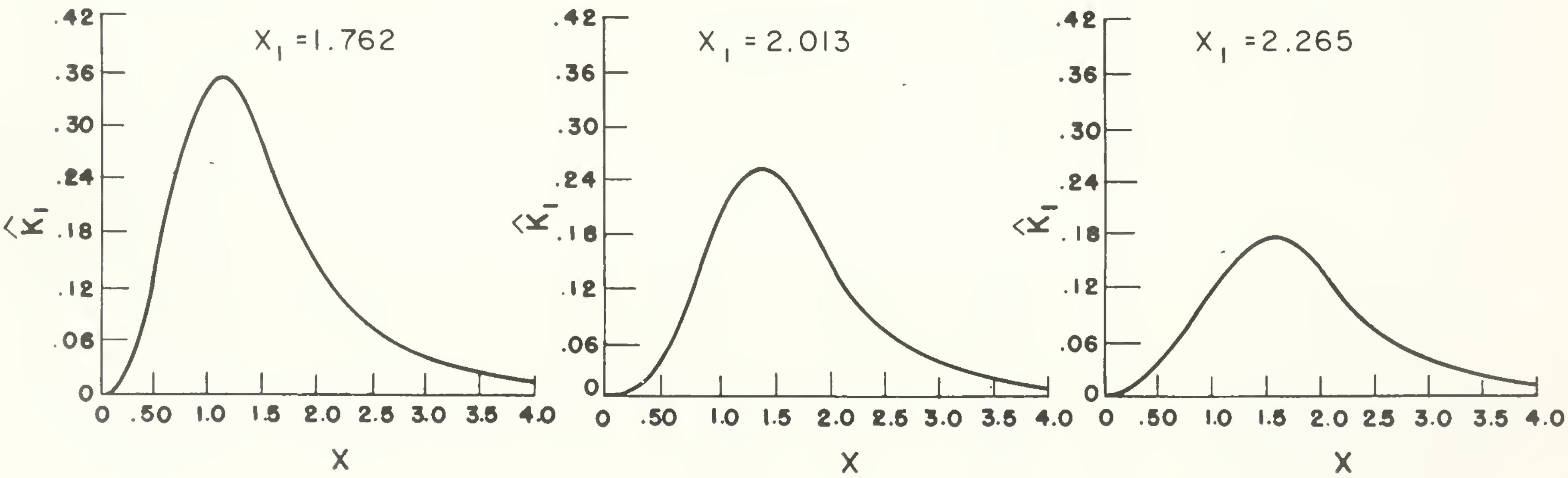
$\hat{K}_1$
$X_1 = 1.762$
$X_1 = 2.013$
$X_1 = 2.265$
X
.42
.36
.30
.24
.18
.12
.06
0
0 .50 1.0 1.5 2.0 2.5 3.0 3.5 4.0

FIG. 2

appear in figure 2, for the corresponding values of x_1.

In other words, the planar, basic climatological flow, W_{cp}, is given by

$$u_{cp} = -\Phi_y \ , \tag{2.22}$$

$$v_{cp} = \Phi_x \ , \tag{2.23}$$

$$h_{cp} = D + \frac{f}{g}\Phi \ , \tag{2.24}$$

where

$$\Phi = -\frac{1}{2\pi}\sum_{i=0}^{3} \gamma_i \hat{K}_o(\kappa\rho_i) \ . \tag{2.25}$$

For a flow with velocity components u and v, the total relative vorticity in a region R is defined by:

$$V(R) \equiv \iint_R (v_x - u_y)dxdy \ . \tag{2.26}$$

Integration by parts yields the formula,

$$V(R) = \oint_{\delta R} udx + vdy \ , \tag{2.27}$$

where the line integral is evaluated on the boundary, δR, of the region R.

Consider the case that the region R is a circle with center at a vortex point, (x_i, y_i), and of radius r_i. Now the distance between any two of the vortex points is either r_p or $\sqrt{3}\, r_p$ (see (2.17)). Hence for the choice

$$\kappa r_i \equiv x_1 = 1.762 < \frac{3.75}{2} ,$$

it is seen that

$$r_i < \frac{r_p}{2} \quad \text{(see (2.17))} .$$

It then follows that for the flow W_{cp} generated by equations (2.22)-(2.25), the derivative of the leading asymptotic term of K_o is used to calculate the total relative vorticity expressed in (2.27); whereas for the flow W_p generated by equations (2.8)-(2.11), the derivative of the function K_o is used in the evaluation of the line integral, (2.27). It follows that, since $K_1(x_1)$ and $\hat{K}_1(x_1) = -g'(x_1)$ differ by less than 9 percent for $x_1 = 1.762^*$, the total relative vorticities, $V(R)$, for the two flows W_{cp} and W_p should differ by about 10 percent for the circle R of radius r_i about (x_i, y_i). Hence the smoothing that produced W_{cp} from W_p did not appreciably change a physically important feature, namely the total relative vorticity associated with the cyclonic and anti-cyclonic regions of the flow.

A description of how the spherical, basic climatological flow, W_c, is constructed from W_{cp} is given in Sections 3-5 for each of the three numerical schemes treated therein. Suffice it to say here that if symmetry of the flow is required, between the northern and southern hemispheres, then it is necessary to smooth the planar flow, W_{cp}, in the neighborhood of the "equator". The equator in the polar tangent plane is taken at a distance approximately equal

---

* $K_o(x_1)$ differs from $g(x_1)$ by less than 6 percent.

to 10,000 km from the origin. Thus the formulas that represent a "symmetrized", planar, climatological flow W_{scp} are defined as follows:

$$u_{scp} = \begin{cases} u_{cp}\ , & \text{for } x^2+y^2 \equiv r^2 \leq d_1^2\ , \\ Q_7(r)u_{cp} + (1-Q_7(r))(-\frac{y}{r})\hat{u}\ , & \text{for } d_1^2 \leq r^2 \leq d_o^2\ , \end{cases}$$

(2.28)
$$v_{scp} = \begin{cases} v_{cp}\ , & \text{for } x^2+y^2 \equiv r^2 \leq d_1^2\ , \\ Q_7(r)v_{cp} + (1-Q_7(r))(\frac{x}{r})\hat{u}\ , & \text{for } d_1^2 \leq r^2 \leq d_o^2\ , \end{cases}$$

$$h_{scp} = \begin{cases} h_{cp}\ , & \text{for } x^2+y^2 \leq d_1^2\ , \\ Q_7(r)h_{cp} + (1-Q_7(r))\hat{h}\ , & \text{for } d_1^2 \leq r^2 \leq d_o^2\ . \end{cases}$$

In other words, up to some distance d_1, from the pole, the symmetrized flow, W_{scp}, is the same as the planar, climatological flow, W_{cp}. Typically d_1 has been chosen to approximate the spherical distance on the earth from the north pole to 4^o north latitude, while d_o approximates the distance from pole to equator. In this band of 4^o width, the planar flow is smoothed by interpolation so that third derivatives of W_{scp} are continuous. That is, $Q_7(r)$ is a polynomial of degree 7 defined by:

(2.29)
$$\begin{cases} Q_7(d_1) = 1\ , \quad Q_7'(d_1) = Q_7''(d_1) = Q_7'''(d_1) = 0\ , \\ Q_7(d_o) = Q_7'(d_o) = Q_7''(d_o) = Q_7'''(d_o) = 0\ . \end{cases}$$

It is easy to verify that

$$0 \leq Q_7(r) \leq 1 \quad \text{for} \quad d_1 \leq r \leq d_o \ .$$

The value $\hat{h}$ is the average value of h_{cp} evaluated on the circle of radius d_o about the origin; while, the value $\hat{u}$ is the average value of the tangential component, $\frac{x}{r} v_{cp} - \frac{y}{r} u_{cp}$, of the velocity (u_{cp}, v_{cp}) evaluated on the circle of radius d_o about the origin. It is easy to verify that the radial component, $\frac{y}{r} v_{scp} + \frac{x}{r} u_{scp}$, of W_{scp} vanishes at $r = d_o$ along with all of its derivatives of order less than 4. In other words, W_{scp}, is approximately a "zonal" or "circular" flow in the immediate vicinity of the "equator", $r = d_o$, with constant height, $\hat{h}$, and with constant tangential component of velocity, $\hat{u}$. It is the flow W_{scp} that is "mapped" onto the northern hemisphere to produce the spherical, climatological flow, W_c, by symmetrization across the equator.

3. The Stereographic Coordinate Scheme, Friction Coefficient, Climatological Flow

3a. Stereographic Coordinates

One of the annoying difficulties, that arises in the numerical solution of hyperbolic equations defined over a complete sphere, is that any spatial coordinate system must have at least one singularity. For example, the spherical coordinate system, with lines of latitude and longitude, is singular at each pole. The natural spatial mesh in spherical coordinates uses uniform intervals in latitude and in longitude. Hence near the poles, the spherical distance between neighborhing mesh points is much smaller than it is, say near the equator. But, the Courant-Friedrichs-Lewy condition, that is necessary for such a difference scheme to be convergent, restricts the ratio of the time step to the smallest space interval. Thus, an inordinately small time step must be used, unless the usual difference methods are altered in regions where the spherical mesh distance is small, i.e. near the poles. In Sections 4 and 5, the use of spatial smoothing operators avoids this restriction of the time step, at the expense of additional calculations in the neighborhood of each pole. A way to avoid having such a singularity in the coordinate system, is to cover the sphere by two overlapping coordinate patches. That is, a spherical latitude region containing the northern hemisphere, say $-8^{\circ} \leq \theta \leq 90^{\circ}$, is mapped stereographically onto a plane tangent at the north pole, by rays emanating from the south pole. An analogous stereographic mapping is carried out for a latitude region

containing the southern hemisphere, say

$$8^\circ \geq \theta \geq -90^\circ ,$$

by projection from the north pole onto a plane tangent at the south pole. The equations of motion are then to be treated in these planar coordinate systems. But, to avoid the natural singularity of polar coordinates in the stereographic planes, the spherical regions are enlarged so that their stereographic images are squares that are tangent to the images of the above described circles of $\pm 8^\circ$ latitude, see figure 3. The stereographic mapping is given by

$$(3.1) \qquad x = am \cos\theta \cos\lambda , \qquad y = am \cos\theta \sin\lambda ,$$

where m, the map factor, is defined by

$$(3.2) \qquad m = \frac{2}{1+\sin\theta} , \qquad -\frac{\pi}{2} < \theta \leq \frac{\pi}{2} ,$$

and the radius of the earth is a. The spherical velocity components (u,v) are defined by

$$(3.3) \qquad u = a\cos\theta\,\dot{\lambda} , \qquad v = a\,\dot{\theta} ;$$

the stereographic velocity components (ϕ,ψ) are defined by

$$(3.4) \qquad \phi = \dot{x} , \qquad \psi = \dot{y} ,$$

where $(\dot{\ }) \equiv \frac{d}{dt}(\ )$ denotes differentiation with respect to time. By differentiating (3.1), the relationship between the two sets of velocity vectors is found:

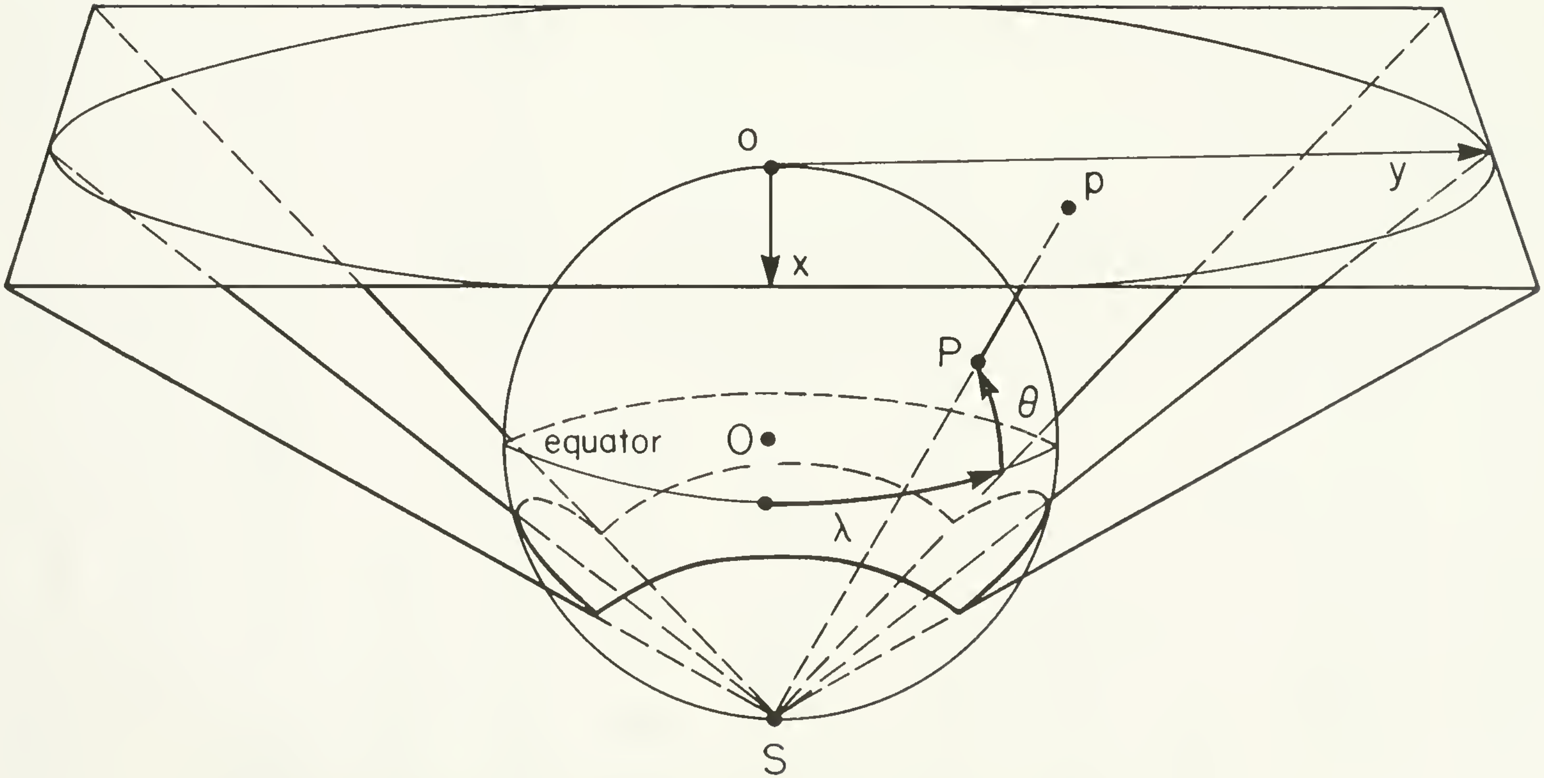

Fig. 3 The stereographic projection of a region encompassing the northern hemisphere, onto a square. The point P, with coordinates (λ,θ) on the sphere, is mapped onto the point p, with coordinates (x,y) in the stereographic plane.

$$(3.5)\qquad \begin{pmatrix} \phi \\ \psi \end{pmatrix} = -mA \begin{pmatrix} u \\ v \end{pmatrix} ,$$

where m is the map factor and A is a rotation matrix,

$$(3.6)\qquad A = \begin{pmatrix} \sin\lambda & \cos\lambda \\ -\cos\lambda & \sin\lambda \end{pmatrix} .$$

The equations of motion, (2.1)-(2.3), become

$$(3.7)\qquad \frac{D}{Dt}\phi - f\psi - \frac{1}{2a^2 m} P_1 + gm^2(m^2H)_x + \frac{R}{m}\phi s = 0 ,$$

$$(3.8)\qquad \frac{D}{Dt}\psi + f\phi - \frac{1}{2a^2 m} P_2 + gm^2(m^2H)_y + \frac{R}{m}\psi s = 0 ,$$

and

$$(3.9)\qquad \frac{\partial}{\partial t} H + (H\phi)_x + (H\psi)_y = 0 ,$$

where

$$\frac{D}{Dt} \equiv \frac{\partial}{\partial t} + \phi\frac{\partial}{\partial x} + \psi\frac{\partial}{\partial y} ,$$

and where the map factor m, and Coriolis parameter $f = 2\Omega\sin\theta$ are expressed in terms of the stereographic coordinates, and along with H, s, P_1, and P_2 are defined by

$$(3.10)\qquad m = \frac{4a^2 + r^2}{4a^2} ; \quad \sin\theta = \frac{4a^2 - r^2}{4a^2 + r^2} , \quad \text{with} \quad r^2 \equiv x^2 + y^2 ;$$

$$H \equiv \frac{h}{m^2} , \qquad s^2 \equiv \phi^2 + \psi^2 ,$$

$$P_1 \equiv x(\phi^2 - \psi^2) + 2y\phi\psi ,$$

$$P_2 = y(\psi^2 - \phi^2) + 2x\phi\psi .$$

Since the area of the stereographic image of a spherical area element is amplified by the factor m^2, the quantity H is proportional to the mass per unit area in the stereographic plane.

3b. Difference Scheme

A difference scheme of second order accuracy in both the time and spatial variables is now constructed. Introduce a uniform mesh spacing in the stereographic square*,

$$x_i = i\Delta x \ , \quad y_j = j\Delta y \tag{3.11}$$

with

$$\Delta x = \Delta y$$

and let the boundaries be given by

$$X = \pm N\Delta x \ , \quad Y = \pm N\Delta y \ . \tag{3.12}$$

Consider any interior mesh point

$$p_1 \equiv (x_i, y_j) \tag{3.13}$$

and its eight neighbors in counter-clockwise order,

$$p_2 \equiv (x_{i+1}, y_j) \ , \quad p_3 \equiv (x_{i+1}, y_{j+1}) \ , \quad p_4 \equiv (x_i, y_{j+1}) \ ,$$

$$p_5 \equiv (x_{i-1}, y_{j+1}) \ , \quad p_6 \equiv (x_{i-1}, y_j) \ , \quad p_7 \equiv (x_{i-1}, y_{j-1}) \ ,$$

$$p_8 \equiv (x_i, y_{j-1}) \ , \quad p_9 \equiv (x_{i+1}, y_{j-1}) \ ,$$ see figure 4 .

* This is equivalent to using an orthogonal circular mesh on the sphere. That is, the lines x = const., y = const. correspond to circles on the sphere.

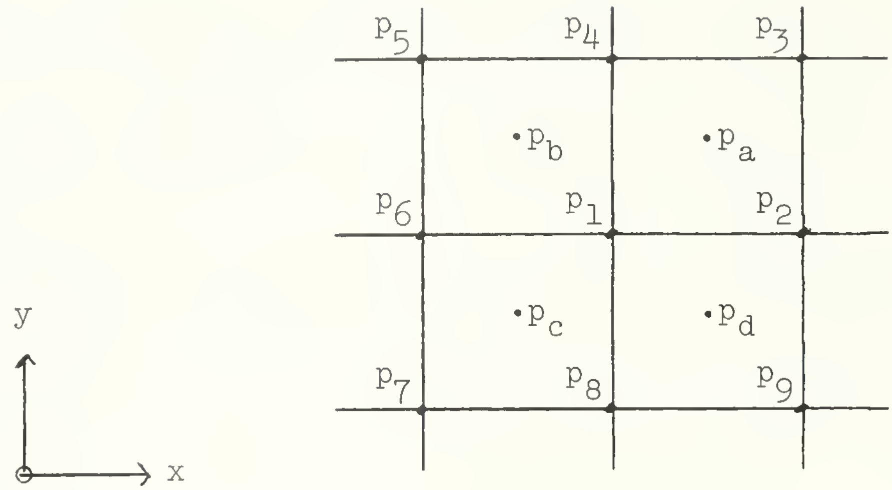

figure 4

The points used in advancing the solution at the interior net point, $p_1 \equiv (x_i, y_j)$

Denote by ϕ_k, ψ_k, H_k, $m_k, \ldots,$ the values of these functions at time t, at the points p_k, $1 \leq k \leq 9$. The scheme finds the values $\phi_1^{t+\Delta t}$, $\psi_1^{t+\Delta t}$, $H_1^{t+\Delta t}$ at time $t+\Delta t$ at p_1, by first predicting tentative values at the centers p_a, p_b, p_c, p_d of the four squares that touch p_1, i.e.

$$
(3.14) \qquad \begin{aligned}
p_a &= \frac{1}{4}(p_1 + p_2 + p_3 + p_4) , \qquad & p_b &= \frac{1}{4}(p_6 + p_1 + p_4 + p_5) , \\
p_c &= \frac{1}{4}(p_7 + p_8 + p_1 + p_6) , \qquad & p_d &= \frac{1}{4}(p_8 + p_9 + p_2 + p_1) .
\end{aligned}
$$

For example, at time t let

$$
(3.15) \qquad \hat{H}_a \equiv \frac{1}{4}(H_1 + H_2 + H_3 + H_4)
$$

and similarly define $\hat{\phi}_a$, $\hat{\psi}_a$, etc. The predicted tentative values at $t+\Delta t$ and p_a, i.e., ϕ_a, ψ_a, H_a are found from the Lax-Friedrichs, first order accurate scheme. Let $\Lambda \equiv \Delta t/\Delta x$, and set

$$(3.16)\quad \phi_a = \hat{\phi}_a - \frac{\Lambda}{2}\{\phi_a[(\phi_2+\phi_3)-(\phi_1+\phi_4)] + \hat{\psi}_a[(\phi_3+\phi_4)-(\phi_2+\phi_1)]$$

$$+ gm_a^2[(m^2H)_2 + (m^2H)_3 - (m^2H)_1 - (m^2H)_4]\}$$

$$+ \Delta t\{f_a\hat{\psi}_a + \frac{1}{2a^2m_a}[x_a(\hat{\phi}_a^2 - \hat{\psi}_a^2) + 2y_a\hat{\phi}_a\hat{\psi}_a] - \frac{R}{m_a}\hat{\phi}_a\hat{s}_a\} ,$$

where $\hat{s}_a^2 = \hat{\phi}_a^2 + \hat{\psi}_a^2$;

$$(3.17)\quad \psi_a = \hat{\psi}_a - \frac{\Lambda}{2}\{\hat{\phi}_a[(\psi_2+\psi_3)-(\psi_1+\psi_4)] + \hat{\psi}_a[(\psi_3+\psi_4)-(\psi_2+\psi_1)]$$

$$+ gm_a^2[(m^2H)_3 + (m^2H)_4 - (m^2H)_2 - (m^2H)_1]\}$$

$$+ \Delta t\{-f_a\hat{\phi}_a + \frac{1}{2a^2m_a}[y_a(\hat{\psi}_a^2 - \hat{\phi}_a^2) + 2x_a\hat{\phi}_a\hat{\psi}_a] - \frac{R}{m_a}\hat{\psi}_a\hat{s}_a\} ;$$

$$(3.18)\quad H_a = \hat{H}_a - \frac{\Lambda}{2}\{[(H\phi)_2 + (H\phi)_3 - (H\phi)_1 - (H\phi)_4]$$

$$+ [(H\psi)_3 + (H\psi)_4 - (H\psi)_2 - (H\psi)_1]\} .$$

Analogous formulas produce tentative values of ϕ_α, ψ_α, H_α, with $\alpha = b, c, d$, at $t + \Delta t$ for the points p_b, p_c, p_d. The averages of the four sets of tentative values, produce first order accurate, tentative values at p_1, namely

$$(3.19)\quad \begin{aligned} \tilde{\phi}_1^{t+\Delta t} &= \frac{1}{4}\sum_{\alpha=a}^{d} \phi_\alpha , \\ \tilde{\psi}_1^{t+\Delta t} &= \frac{1}{4}\sum_{\alpha=a}^{d} \psi_\alpha . \end{aligned}$$

Finally, the values at $t + \Delta t$ and p_1, i.e., $\phi_1^{t+\Delta t}$, $\psi_1^{t+\Delta t}$, and $H_1^{t+\Delta t}$, are determined by a second order accurate, "corrector" type

formula (analogous to Burstein's version of Richtmyer's two-step, Lax-Wendroff scheme):

(3.20)

$$\phi_1^{t+\Delta t} = \phi_1 - \frac{\Lambda}{4}\Big\{\phi_1(\phi_2 - \phi_6) + \psi_1(\phi_4 - \phi_8) + gm_1^2[(m^2H)_2 - (m^2H)_6]$$

$$+ \tilde{\phi}_1^{t+\Delta t}[(\phi_d + \phi_a) - (\phi_c + \phi_b)] + \tilde{\psi}_1^{t+\Delta t}[(\phi_a + \phi_b) - (\phi_d + \phi_c)]$$

$$+ gm_1^2[(m_d^2H_d + m_a^2H_a) - (m_c^2H_c + m_b^2H_b)]\Big\}$$

$$+ \frac{\Delta t}{2}\Big\{f_1(\psi_1 + \tilde{\psi}_1^{t+\Delta t}) + \frac{1}{2a^2m_1}[x_1(\phi_1^2 - \psi_1^2 + (\tilde{\phi}_1^{t+\Delta t})^2 - (\tilde{\psi}_1^{t+\Delta t})^2)$$

$$+ 2y_1(\phi_1\psi_1 + \tilde{\phi}_1^{t+\Delta t}\ \tilde{\psi}_1^{t+\Delta t})] - \frac{R}{m_1}\ (\phi_1 s_1 + \tilde{\phi}_1^{t+\Delta t}\ \tilde{s}_1^{t+\Delta t})\Big\} \quad ,$$

where $(\tilde{s}_1^{t+\Delta t})^2 = (\tilde{\phi}_1^{t+\Delta t})^2 + (\tilde{\psi}_1^{t+\Delta t})^2$;

(3.21)

$$\psi_1^{t+\Delta t} = \psi_1 - \frac{\Lambda}{4}\Big\{\phi_1(\psi_2 - \psi_6) + \psi_1(\psi_4 - \psi_8) + gm_1^2[(m^2H)_4 - (m^2H)_8]$$

$$+ \tilde{\phi}_1^{t+\Delta t}[\psi_d + \psi_a - \psi_c - \psi_b] + \tilde{\psi}_1^{t+\Delta t}[\psi_a + \psi_b - \psi_d - \psi_c]$$

$$+ gm_1^2[m_a^2H_a + m_b^2H_b - m_d^2H_d - m_c^2H_c]\Big\}$$

$$+ \frac{\Delta t}{2}\Big\{-f_1(\phi_1 + \tilde{\phi}_1^{t+\Delta t}) + \frac{1}{2a^2m_1}[y_1(\psi_1^2 - \phi_1^2 + (\tilde{\psi}_1^{t+\Delta t})^2 - (\tilde{\phi}_1^{t+\Delta t})^2)$$

$$+ 2x_1(\phi_1\psi_1 + \tilde{\phi}_1^{t+\Delta t}\ \tilde{\psi}_1^{t+\Delta t})] - \frac{R}{m_1}\ (\psi_1 s_1 + \tilde{\psi}_1^{r+\Delta t}\ \tilde{s}_1^{t+\Delta t})\Big\} \quad ;$$

(3.22) $$H_1^{t+\Delta t} = H_1 - \frac{\Lambda}{4}\ [(H\phi)_2 - (H\phi)_6 + (H_d\phi_d + H_a\phi_a) - (H_c\phi_c + H_b\phi_b)$$

$$+ (H\psi)_4 - (H\psi)_8 + (H_a\psi_a + H_b\psi_b) - (H_d\psi_d + H_c\psi_c)] \ .$$

The values of ϕ, ψ, and H at the boundary points of the northern stereographic square are found at $t+\Delta t$ by interpolation in the values at $t+\Delta t$ for the interior points of the southern stereographic square. That is, the mapping of the southern region with rectangular coordinates $(\overline{x},\overline{y})$ is defined by

$$\overline{x} = an \cos\theta \cos\lambda \, , \quad \overline{y} = an \cos\theta \sin\lambda \, , \tag{3.23}$$

where the map factor, n, satisfies

$$\begin{aligned} n &= \frac{2}{1-\sin\theta} \, , \quad -\frac{\pi}{2} \leq \theta < \frac{\pi}{2} \, ; \\ \sin\theta &= \frac{\overline{r}^2 - 4a^2}{4a^2+\overline{r}^2} \, , \quad \overline{r}^2 = \overline{x}^2+\overline{y}^2 \, . \end{aligned} \tag{3.24}$$

From (3.3), (3.23) and (3.24), it follows that the velocity components

$$\overline{\phi} \equiv \dot{\overline{x}} \, , \quad \overline{\psi} \equiv \dot{\overline{y}} \tag{3.25}$$

satisfy

$$\begin{pmatrix} \overline{\phi} \\ \overline{\psi} \end{pmatrix} = nB \begin{pmatrix} u \\ v \end{pmatrix} \, , \tag{3.26}$$

where B is the rotation matrix

$$B = \begin{pmatrix} -\sin\lambda & \cos\lambda \\ \cos\lambda & \sin\lambda \end{pmatrix} . \tag{3.27}$$

Furthermore, the variable

$$\overline{H} = \frac{h}{n^2} \, , \tag{3.28}$$

is proportional to the mass per unit area in the southern stereographic plane.

The equations of motion, for the southern stereographic plane, are identical to the equations (3.7)-(3.10) with (ϕ,ψ,H,x,y,m,f) replaced by $(\overline{\phi},\overline{\psi},\overline{H},\overline{x},\overline{y},n,-f)$, but with $\sin\theta$ defined by (3.24). Hence the difference equations for the advance of $\overline{\phi}$, $\overline{\psi}$, $\overline{H}$ at interior points of the southern mesh $(\overline{x}_i,\overline{y}_j)$ are identical in form, to those for the northern mesh. But, each boundary point p of the northern square corresponds to some point P on the sphere, whose representative $\overline{p}$ lies well in the interior of the southern square and vice-versa. Now when a point P on the sphere corresponds to $p \equiv (x,y)$ a point of the northern stereographic square, then the point P corresponds to the point $\overline{p} \equiv (\overline{x},\overline{y})$ in the southern stereographic square, with

$$(3.29) \qquad \overline{p} = \frac{n}{m}p \ , \qquad \frac{n}{m} = \frac{1+\sin\theta}{1-\sin\theta} = \frac{4a^2}{x^2+y^2} \ .$$

Therefore, if p is a mesh point of the northern plane, it is unlikely that $\overline{p}$, given by (3.29), is a mesh point of the southern plane. In fact, for $N \geq 16$, any northern boundary mesh point, p, when plotted at its position $\overline{p}$ in the southern stereographic plane is surrounded by 16 interior mesh points of the southern plane, see figure 5. The functions $\overline{\phi}$, $\overline{\psi}$ and $\overline{H}$ are known at the mesh points $\overline{p}_k$, $1 \leq k \leq 16$, that surround $\overline{p}$. The sixteen-point Lagrange interpolation formula of the form

$$(3.30) \qquad \overline{\phi}(\overline{p}) = \sum_{k=1}^{16} \omega_k(\overline{p})\overline{\phi}(\overline{p}_k)$$

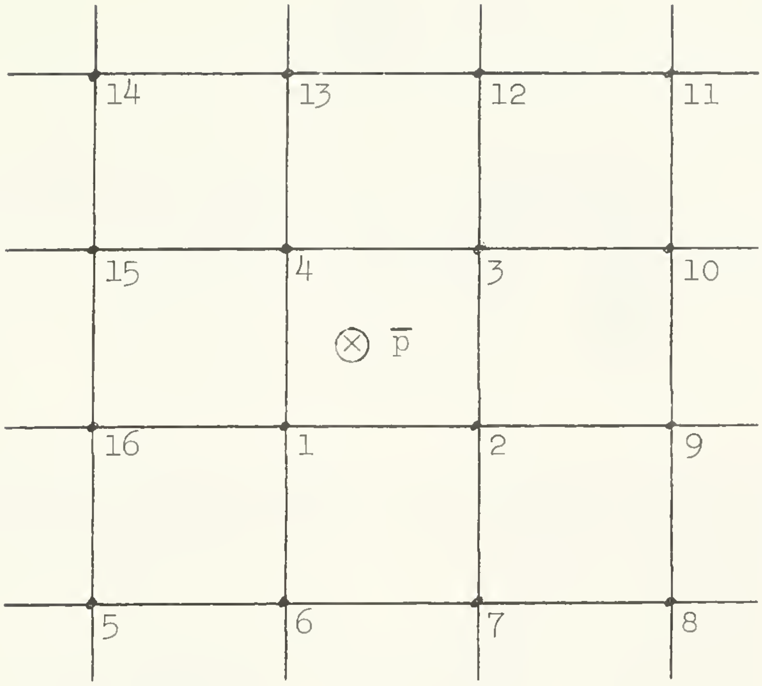

figure 5

In the southern stereographic plane, the point $\overline{p}$, corresponding to a boundary point of the northern mesh, is surrounded by sixteen interior points

is correct for cubic polynomials. With $\omega_k = 0$ for $k = 5, 6, \ldots, 16$, the corresponding four-point Lagrange interpolation polynomial is correct for linear polynomials.

After finding $\overline{\phi}(\overline{p})$, $\overline{\psi}(\overline{p})$, $\overline{H}(\overline{p})$ by interpolation, the quantities $\phi(p)$, $\psi(p)$ are obtained from (3.5) and (3.26), that is,

$$(3.31) \qquad \begin{pmatrix} \phi \\ \\ \psi \end{pmatrix} = -\frac{m}{n} AB^{-1} \begin{pmatrix} \overline{\phi} \\ \\ \overline{\psi} \end{pmatrix} ;$$

while H(p) is found from (3.9) and (3.28) in the form

(3.32) $$H = \frac{n^2}{m^2} \overline{H} ,$$

where (3.29) is used and it is easy to verify that

$$AB^{-1} = \begin{pmatrix} \cos 2\lambda & \sin 2\lambda \\ \sin 2\lambda & -\cos 2\lambda \end{pmatrix} .$$

The predictor-corrector type difference equations (3.16)-(3.22) were developed to solve the initial-value problem for the homogeneous system of differential equations (3.7)-(3.9). Let the system of three differential equations be denoted by

(3.33) $$L(W) = 0 ,$$

where W is three component vector (ϕ, ψ, H) and L is a vector with three components, (L_1, L_2, L_3), that represent the left sides of equations (3.7)-(3.9) respectively. Consider the corresponding non-homogeneous system

(3.34) $$L(W) = Z ,$$

where Z has the three components (E,F,G) that are prescribed functions of (x,y,t). The system (3.34) may be solved numerically by using a natural modification of the right-hand sides of formulas (3.16)-(3.18) and (3.20)-(3.22), as follows:

$$
\begin{aligned}
&\text{In (3.16), add } \Delta t E_a(t) \;; \\
&\text{in (3.17), add } \Delta t F_a(t) \;; \\
&\text{in (3.18), add } \Delta t G_a(t) \;; \\
&\text{in (3.20), add } \Delta t E_1(t+\tfrac{\Delta t}{2}) \;; \\
&\text{in (3.21), add } \Delta t F_1(t+\tfrac{\Delta t}{2}) \;; \\
&\text{in (3.22), add } \Delta t G_1(t+\tfrac{\Delta t}{2}) \;.
\end{aligned}
\tag{3.35}
$$

The solution of the finite difference equation (3.35) is denoted by W_Δ.

3c. Friction Coefficient, Spin-down Time

Varying the friction coefficient R, will affect the rate at which a solution of the initial value problem for the homogeneous system (3.7)-(3.9) (or equivalently (3.33)) tends to lose kinetic energy. Numerical experiments using (3.16)-(3.22) were performed for initial data that corresponded to the purely zonal flow given by (2.5), with $a = 6.37\times 10^8$cm; $D = 8.5\times 10^5$cm; $Q = 500\ \frac{\text{cm}}{\text{sec}}$, $1000\ \frac{\text{cm}}{\text{sec}}$; $R = 0.5\times 10^{-7}\ \frac{1}{\text{cm}}$, $1.0\times 10^{-7}\ \frac{1}{\text{cm}}$. (For the choice R = 0, the purely zonal flow is an exact solution of (3.7)-(3.9).) The region of the northern stereographic plane consisted of a square that circumscribed the image of the circle at -8° latitude on the sphere. The interval sizes were $\Delta x = \Delta y = \frac{1}{32}$ side of square $\cong 0.916\times 10^8$, $\Delta t = 690$ sec.

Figure 6 contains graphs of the maximum speed on the sphere, $\sqrt{u^2+v^2}$, as a function of the time, for these four cases. For the larger coefficient of friction, the maximum speed levels off after

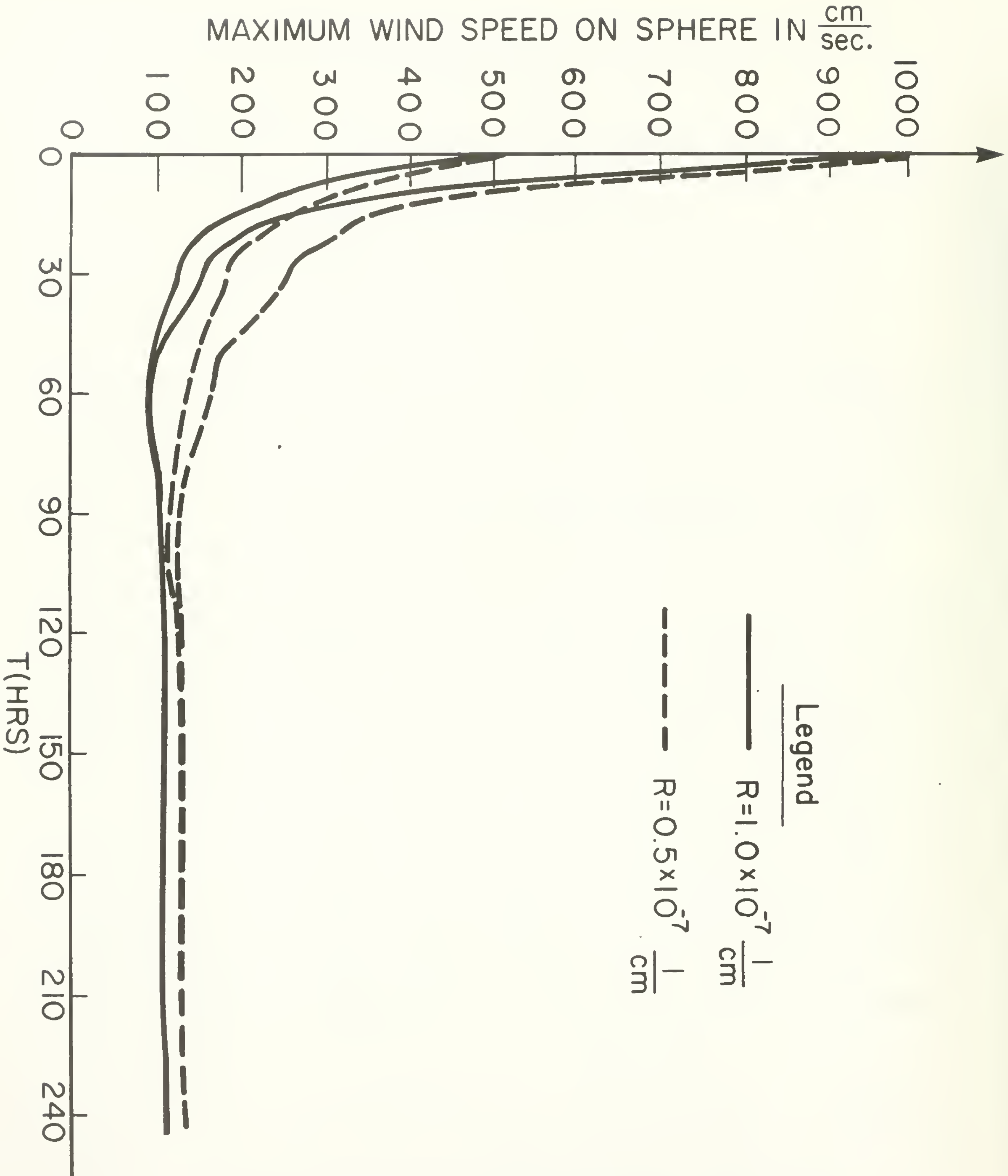

Fig. 6 Decay of the maximum velocity in zonal flow for different friction coefficients in the stereographic coordinates scheme.

about 5 days, to a value that is about 115 $\frac{\text{cm}}{\text{sec}}$; whereas for the smaller coefficient of friction, the maximum speed levels off after about $6\frac{1}{2}$ days, to a value that is about 140 $\frac{\text{cm}}{\text{sec}}$. Both the value of the limiting maximum speed and the time at which it is attained, seem not to depend on the initial speed but do depend on the friction coefficient. The time required to reach the limiting maximum speed may be thought of as being the spin-down time.

3d. Climatological Flows

A natural way to test the accuracy of a long-term integration produced by (3.35) is to treat the system (3.34), with the non-homogeneous term chosen to have the special form

$$Z \equiv L(W_c) \ ,$$

where W_c is some prescribed function. For example, one such choice that was tried is

$$W_c \equiv (\phi_c, \psi_c, H_c) \ ,$$

with

$$\phi_c \equiv u_{scp} \ , \quad \psi_c \equiv v_{scp} \ , \quad m^2 H_c \equiv h_c \equiv h_{scp} \ ,$$

where the symmetrized, planar climatological flow variables are defined in (2.28). Here the centers of the three anti-cyclonic cells are initially placed 120° apart on a circle of radius r_p in the stereographic square that corresponds to a latitude of about 30.78°,

$$r_p = \sqrt{x^2 + y^2} \cong 7.24 \times 10^8 \ .$$

Plots of the contour lines of h_c, $H_c \equiv h_c/m^2$, $H_c - D/m^2$, $q \equiv \sqrt{u^2 + v^2}$, ϕ_c, and ψ_c are drawn in figs. 7, 8a, 8b, 9, 10 and 11 respectively, for the parameter values $D = 8.5 \times 10^5$cm, $\gamma_o = -.0816\gamma_i$, $\gamma_i = -4 \times 10^{12}$ cm^2/sec for i = 1,2,3; $x_1 = 1.762$, $b = 3.262$, $d_o = 12.74 \times 10^8$, $d_1 = 11.91 \times 10^8$, $\hat{h} = 8.517 \times 10^5$cm, $\hat{u} = -65.7$ where $d_o \cong 2a$ is approximately twice the radius of the earth in centimeters. The solution W_Δ of (3.35) with initial data $W_\Delta = W_c$ was computed for several days, while the forcing function $Z = L(W_c)$ was held steady, i.e. W_c was constant in time. The finite difference solution W_Δ settled to a steady state in about 30 hours; a plot of the steady contours of $h_\Delta \equiv m^2 H_\Delta$, is shown in fig. 12. Since $W \equiv W_c$ is the solution of (3.34), the discrepancy $h_\Delta - h_c$ is a result of the truncation error based on the use of: a 33×33 spatial net point mesh for the stereographic square, the corresponding time interval $\Delta t = 690$ sec, and interpolation to find the boundary values. This discrepancy is analogous to the initialization error that arises when using real initial data in a global circulation model (see the report IMM-400 by M. Ghil listed in Section 6).

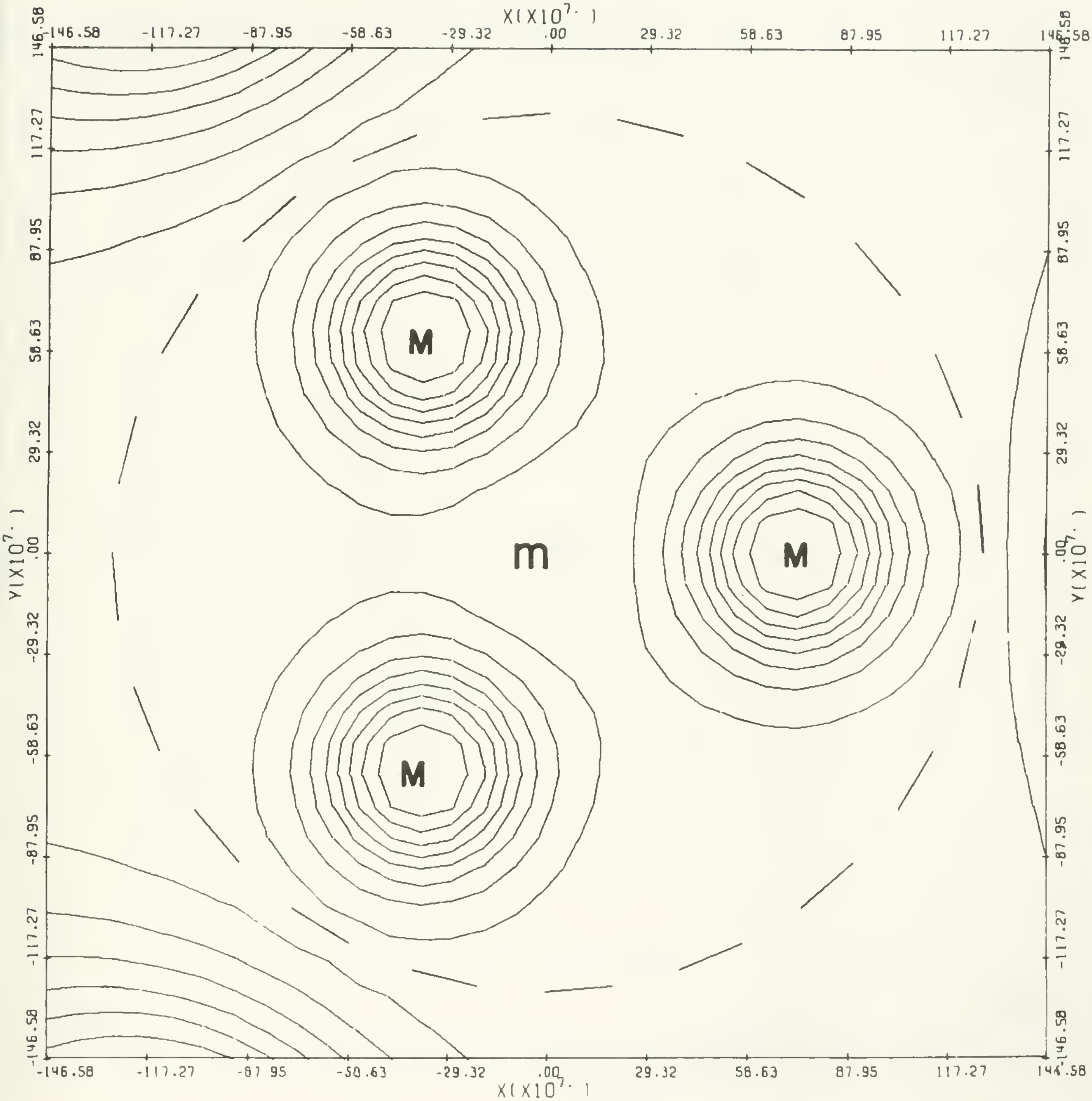

Fig. 7 Contours of the initial height field h_o, plotted in the northern stereographic square. The equator is represented by the dashed circle. Maximum value of $h_o = .90 \times 10^6$ cm = M; minimum value of $h_o = .85 \times 10^6$ cm = m, contour interval = $.554 \times 10^4$ cm. The three highs are centered at 30°N latitude and are 120° apart in longitude. The low is centered at the pole.

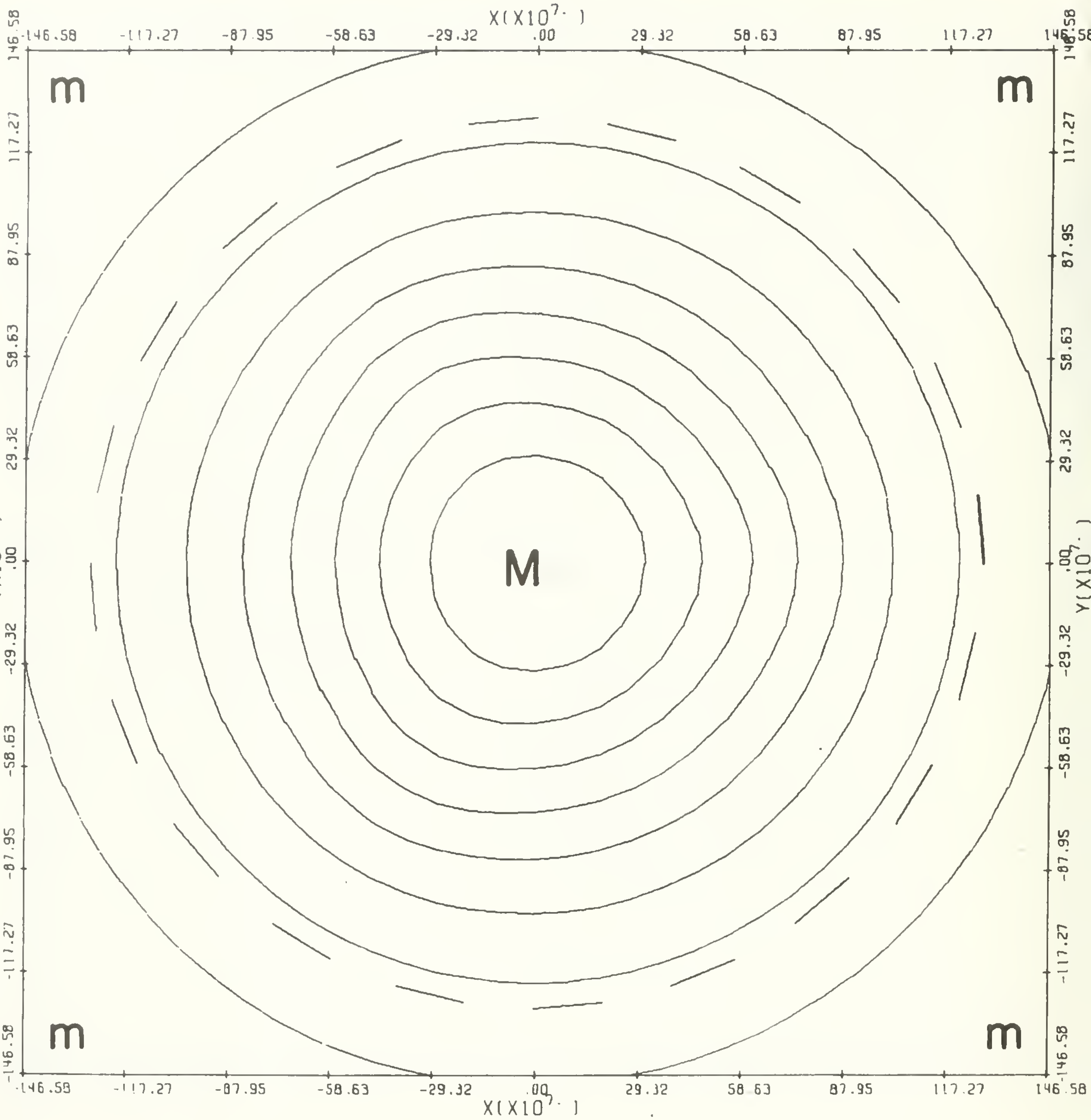

Fig. 8A Contours of the initial height field H_o, plotted in the northern stereographic square (since $H_o = h_o/m^2$, the variation of the area factor m^2 primarily determines the shape of the contours). Maximum value of $H_o = .85 \times 10^6$ = **M**, minimum value of $H_o = 642 \times 10^5$ = m, contour interval = $.873 \times 10^5$. The equator is represented by the dashed circle.

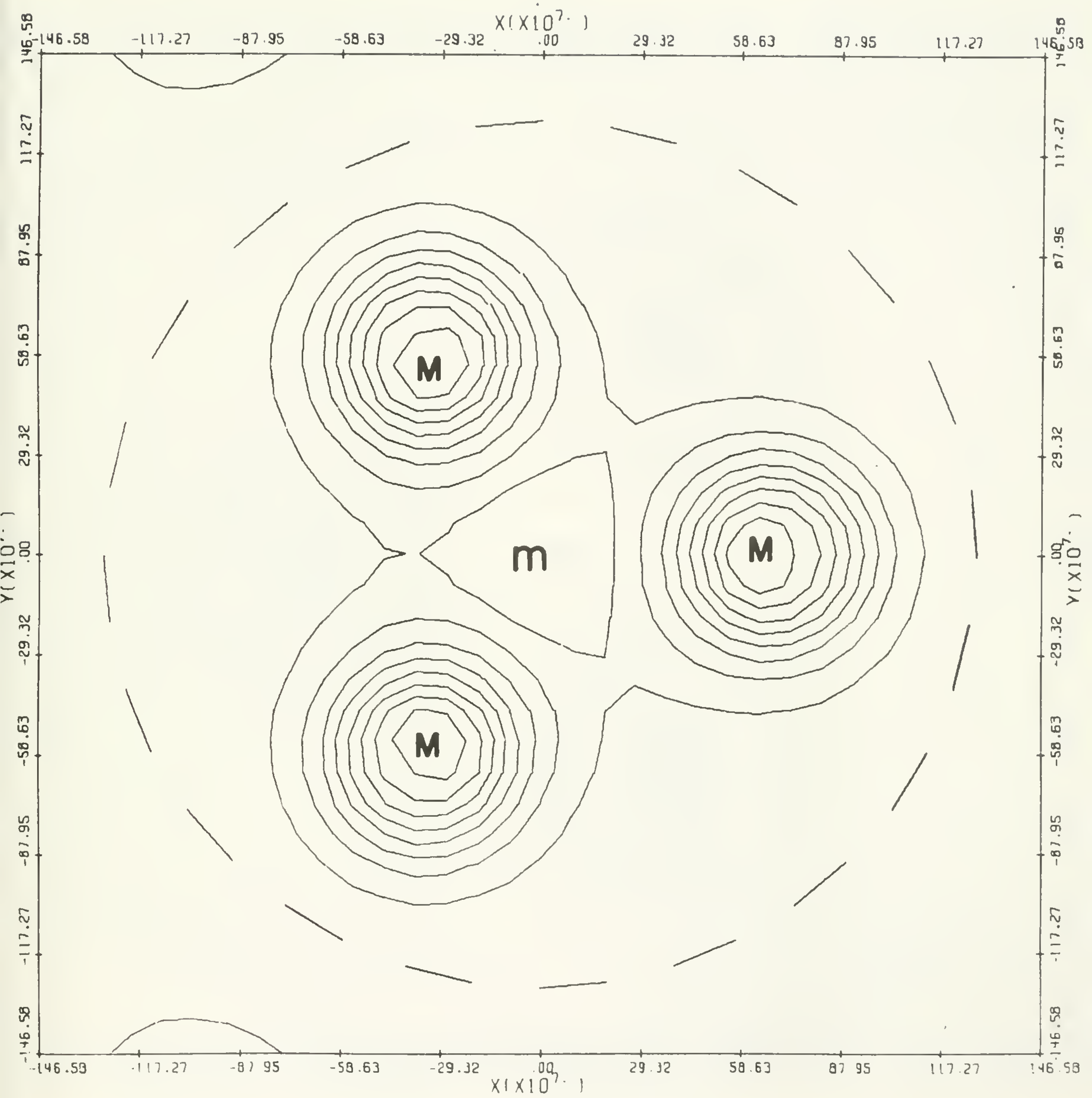

Fig. 8B Contours of the modified initial height field $H_o - D/m^2$, with $D = .85 \times 10^6$, plotted in the northern stereographic square. Maximum value of $H_o - D/m^2 = .313 \times 10^5 =$ **M**, minimum value of $H_o - D/m^2 = .102 \times 10^3 =$ **m**, contour interval $= .347 \times 10^4$. The equator is represented by the dashed circle.

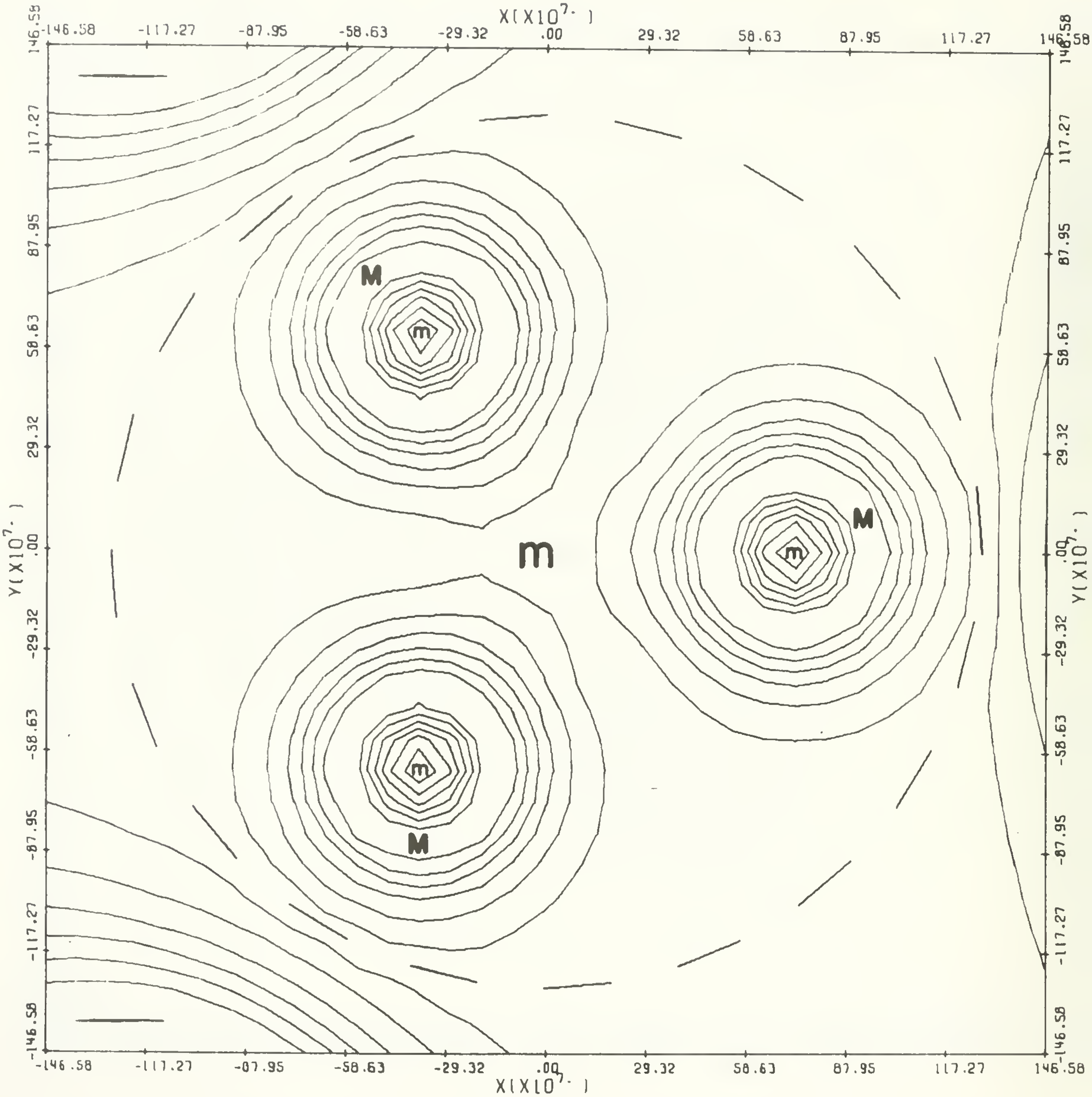

Fig. 9 Contours of the initial wind speed $q = \sqrt{u^2 + v^2}$, plotted in the northern stereographic square. Maximum speed $= .116 \times 10^4 \ \frac{cm}{sec} = M$, minimum speed $= .59 \times 10^{-8} \ \frac{cm}{sec} = m$, contour interval $= .166 \times 10^3 \ \frac{cm}{sec}$. The equator is represented by the dashed circle.

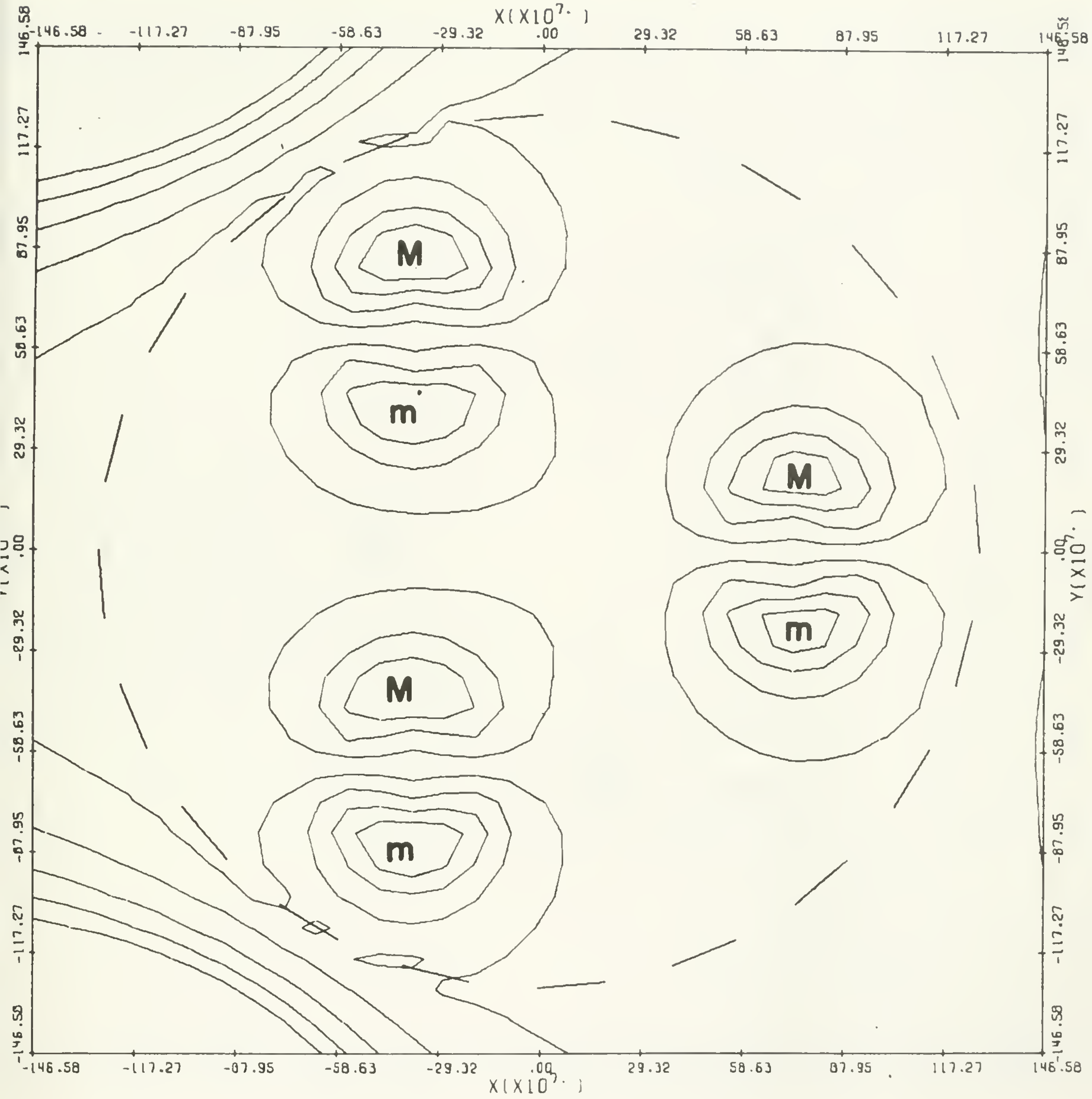

Fig. 10 Contours of the initial velocity component ϕ, plotted in the northern stereographic square. Maximum value of $\phi = .167 \times 10^4 =$ M, minimum value of $\phi = -.167 \times 10^4 =$ m, contour interval $= .371 \times 10^3$. The equator is represented by the dashed circle.

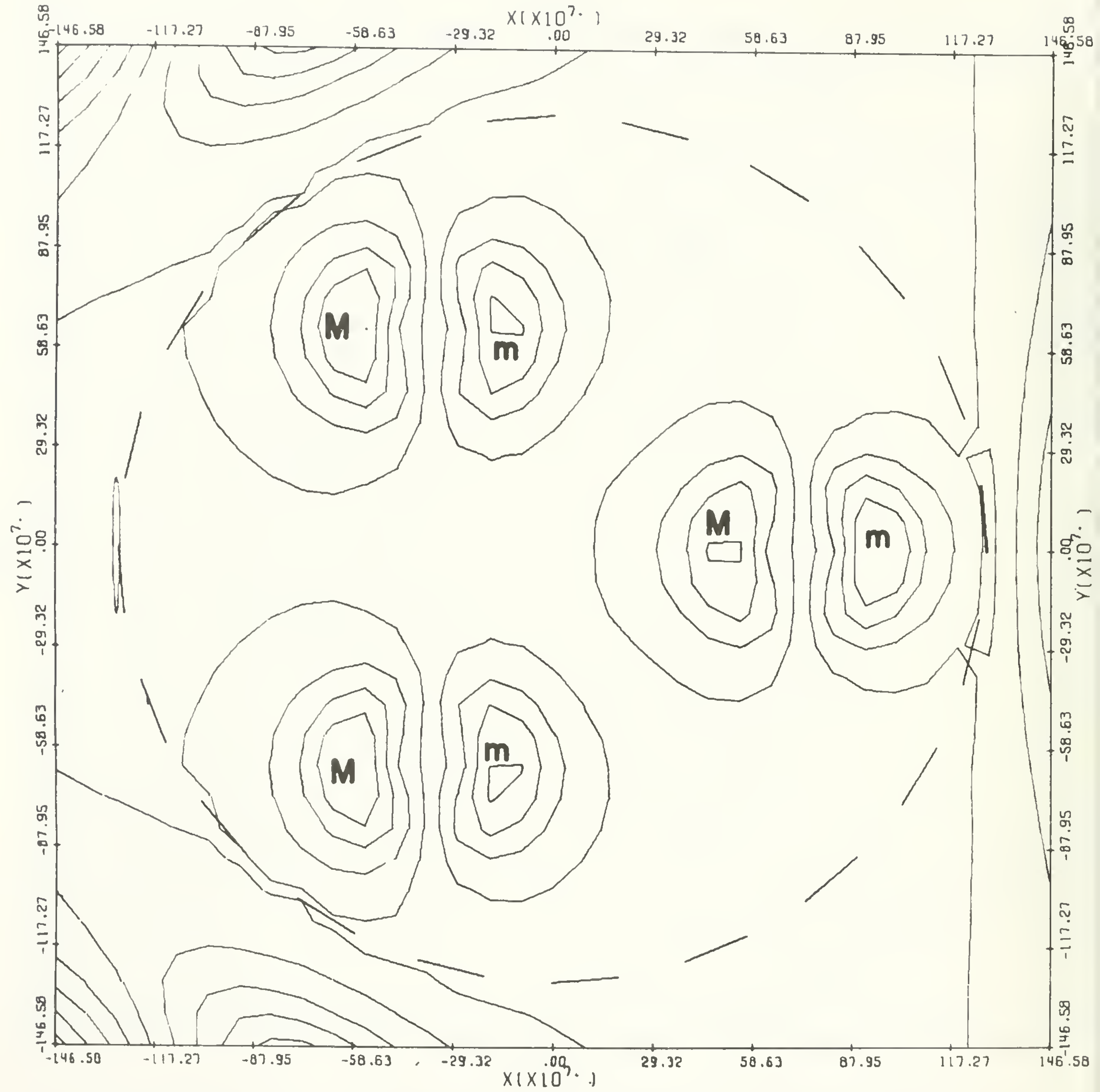

Fig. 11 Contours of the initial velocity component ψ, plotted in the northern stereographic square. Maximum value of $\psi = .164 \times 10^4$ = **M**, minimum value of $\psi = -.165 \times 10^4$ = **m**, contour interval $= .355 \times 10^3$. The equator is represented by the dashed circle.

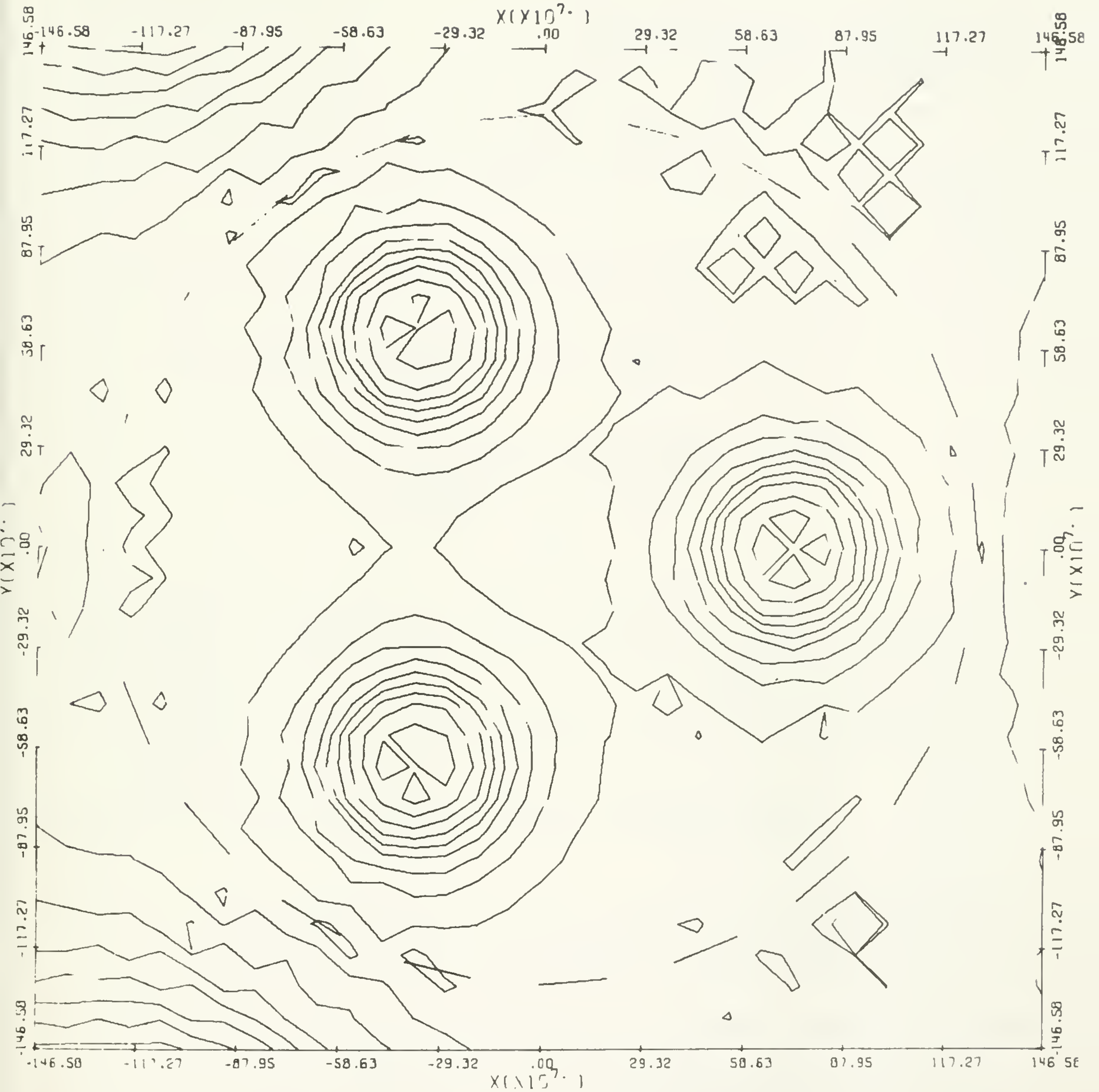

Fig. 12 Contours of the height field h_Δ, produced after 49 hours by solving the difference equations in the stereographic coordinates. Contours of the initial height data h_o are plotted in Fig. 7 at the same interval. The truncation error of the scheme produces the non-zero difference of $h_\Delta - h_o$.

4. A Mintz-Arakawa Type Scheme

4a. Difference Scheme

The Mintz-Arakawa type scheme is based on the conservation of mass equation (2.3) and the momentum form of equations (2.1), (2.2); namely,

$$(4.1) \qquad \frac{\partial}{\partial t}(hu) + \frac{1}{a \cos \theta}\left[\frac{\partial}{\partial \lambda}(hu^2) + \frac{\partial}{\partial \theta}(huv \cos \theta)\right] - \left(f + \frac{u}{a}\tan \theta\right)hv + \frac{gh}{a \cos \theta}\frac{\partial h}{\partial \lambda} + Rhuq = 0 ,$$

$$(4.2) \qquad \frac{\partial}{\partial t}(hv) + \frac{1}{a \cos \theta}\left[\frac{\partial}{\partial \lambda}(huv) + \frac{\partial}{\partial \theta}(hv^2 \cos \theta)\right] + \left(f + \frac{u}{a}\tan \theta\right)hu + \frac{gh}{a}\frac{\partial h}{\partial \theta} + Rhvq = 0 ,$$

where $q^2 \equiv u^2 + v^2$. A spatially staggered, longitude-latitude net is used with a simple predictor-corrector procedure to advance the solution at each time step. The scheme is second order accurate in the spatial increment and first order accurate in the time interval. This process does not use a cycle of five different predictor-corrector steps as is used in the Mintz-Arakawa General Circulation Model [4].

The longitude-latitude mesh is based on intervals $\Delta\lambda = 5^\circ$, $\Delta\theta = 4^\circ$. The equator is a latitudinal mesh line, and the poles are thus 2° away from their nearest latitudinal mesh lines. The velocity components (u, v) are calculated at the intersections of the mesh lines. The value of h is computed at the "midpoint" of each cell in the (λ, θ) plane and also at each pole. The integer indices (i, j) may be used to denote the points of intersection of the mesh lines where $1 \leq i \leq I = 72$, $1 \leq j \leq J = 45$. In this

representation the points $(1,j)$ and $(73,j)$ are identical, for $1 \leq j \leq J$; while the points $(i,23)$ lie on the equator. The lengths of the sides of a mesh cell are given by

$$\alpha = a \cos \theta \Delta\lambda \ , \quad \beta = a\Delta\theta \ , \tag{4.3}$$

in the longitudinal and latitudinal directions respectively. When (i,j) denotes the northeast corner of a cell, (u_{ij}, v_{ij}) denotes the velocity vector at the northeast corner of that cell, while h_{ij} denotes the value of the height of the layer at the "center" of that cell in (λ, θ) coordinates (see fig. 13).

It is convenient to introduce the variable

$$\mathcal{H}_{ij} \equiv \alpha\beta h \tag{4.4}$$

to represent the mass in this cell, when both α and h are calculated at the center of the cell. On the other hand, the mass flux per unit time through the north side of the cell is denoted by

$$V^*_{ij} = \alpha \frac{(v_{i-1,j} + v_{i,j})}{2} \cdot \frac{(h_{i,j} + h_{i,j+1})}{2} \ , \tag{4.5}$$

where α is evaluated at the latitude of the north side of the cell; while the mass flux per unit time through the east side of the cell is denoted by

$$U^*_{ij} = \beta \frac{(h_{i,j} + h_{i+1,j})}{2} (u_{i,j})_{\text{average}} \ . \tag{4.6}$$

Here, the formula for the average value of $u_{i,j}$, depends on the latitude line j. That is, if $(u_{i,j})_{\text{average}}$ were defined to be

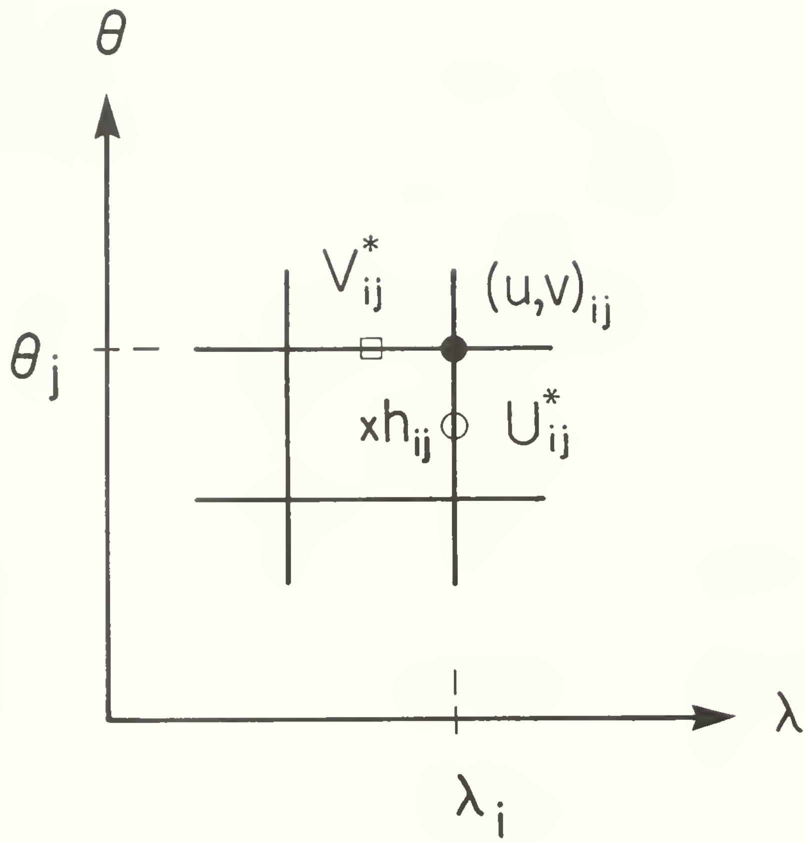

Fig. 13 The locations at which the quantities with subscripts i, j are centered.

$$(u_{i,j})_{\text{average}} \equiv u_{i,j}^{(0)} \equiv \frac{(u_{i,j} + u_{i,j-1})}{2} ,$$

then a quite small time step would be required to ensure the stability of the difference scheme (by the Courant-Friedrichs-Lewy condition). To overcome this restriction of the time step, the Mintz-Arakawa scheme [4] introduces smoothing to compute the fluxes $U^*_{i,j}$, that is the average value of the velocity is defined by

$$(4.7) \qquad (u_{i,j})_{\text{average}} \equiv u_{i,j}^{(N_j)} ,$$

where

$$u_{i,j}^{(0)} = \frac{u_{i,j} + u_{i,j-1}}{2} ,$$

$$u_{i,j}^{(k)} = u_{i,j}^{(k-1)} + \kappa_j (u_{i-1,j}^{(k-1)} - 2u_{i,j}^{(k-1)} + u_{i+1,j}^{(k-1)}) , \quad 1 \leq k \leq N_j .$$

Here the number of smoothings N_j and the smoothing coefficients κ_j are functions of the latitude (the formulas defining κ_j and N_j are given in equation (4.20), see [4]). $N_j = 0$ for lines of latitude near the equator. The interval size $\Delta t = 6$ minutes is now used.

Let the zero right-hand sides of the equations (4.1), (4.2) and (2.3) be replaced by the functions F, G and Q respectively. The difference scheme for predicting the value at $t + \Delta t$ of the mass $\mathcal{H}_{i,j}$, for $2 \leq j \leq J$ is found by computing the mass flux across the boundary of the cell and the contribution from the source term Q:

$$(4.8) \quad \hat{\mathcal{H}}_{i,j}^{t+\Delta t} = \mathcal{H}_{i,j}^{t} + \Delta t \left[(U_{L-1,j}^{*t} - U_{i,j}^{*t}) + (V_{L,j-1}^{*t} - V_{i,j}^{*t}) + (\alpha\beta Q)_{i,j}^{t} \right] ,$$

where α and Q are evaluated at the center of the cell having indices (i,j) at its northeast corner. At the poles, h_1 and h_{J+1} are the values of the height of the layer. Since the surface area γ of the polar caps bounded by the lines of latitude corresponding to $j = 1$ and $j = J$ is given by

$$(4.9) \qquad \gamma = 4\pi a^2 \sin^2 \frac{\Delta\theta}{4} ,$$

the mass of the layer for each of the polar caps may be represented by

$$(4.10) \qquad \mathcal{H}_1 = \gamma h_1 , \quad \mathcal{H}_{J+1} = \gamma h_{J+1} .$$

The rate of change of mass per unit time in the northern polar cap is given by the sum of the fluxes $V^*_{i,J}$ around the northern most circle of latitude. Therefore the formula for predicting the value of $\mathcal{H}_{J+1}$ at $t + \Delta t$ is:

$$(4.11) \qquad \hat{\mathcal{H}}^{t+\Delta t}_{J+1} = \mathcal{H}^{t}_{J+1} + \Delta t \alpha \sum_{i=1}^{I} V^*_{i,J} ,$$

where α is evaluated on the latitude circle $j = J$. The corresponding formula for the southern polar cap is

$$(4.12) \qquad \hat{\mathcal{H}}^{t+\Delta t}_{1} = \mathcal{H}^{t}_{1} - \Delta t \alpha \sum_{i=1}^{I} V^*_{i,1}$$

where α is evaluated on the latitude circle $j = 1$.

Formulas (4.8), (4.11), and (4.12) can be considered to be of the form

$$(4.13) \qquad \hat{\mathcal{H}}^{t+\Delta t} = \mathcal{H}^{t} + \Delta t [\frac{\partial \mathcal{H}}{\partial t}]^{t} .$$

The equations (4.1) and (4.2) (with right-hand sides F and G) are next used to produce predicted values of $\mathcal{H}u$ and $\mathcal{H}v$ at $t+\Delta t$, in the form

$$(4.14)\qquad \begin{aligned} (\widehat{\mathcal{H}u})^{t+\Delta t} &= (\mathcal{H}u)^{t} + \Delta t\left[\frac{\partial(\mathcal{H}u)}{\partial t}\right]^{t} , \\ (\widehat{\mathcal{H}v})^{t+\Delta t} &= (\mathcal{H}v)^{t} + \Delta t\left[\frac{\partial(\mathcal{H}v)}{\partial t}\right]^{t} . \end{aligned}$$

That is, after multiplying (4.1) and (4.2) by $\alpha\beta$, the rate of change $\frac{\partial(\mathcal{H}u)}{\partial t}$ and $\frac{\partial(\mathcal{H}v)}{\partial t}$ may be determined when the derivatives $\frac{\partial}{\partial\lambda}$ and $\frac{\partial}{\partial\theta}$ are replaced by $\frac{\partial}{\partial i}$ and $\frac{\partial}{\partial j}$, respectively in the longitudinal and latitudinal directions, as follows:

$$(4.15)\qquad \frac{\partial(\mathcal{H}u)}{\partial t} + \frac{\partial}{\partial i}(U^{*}u) + \frac{\partial}{\partial j}(V^{*}u) - \alpha\beta hv\left(f + \frac{u\tan\theta}{a}\right) + g\beta h\frac{\partial h}{\partial i} + R\alpha\beta huq = \alpha\beta F ,$$

$$(4.16)\qquad \frac{\partial(\mathcal{H}v)}{\partial t} + \frac{\partial}{\partial i}(U^{*}v) + \frac{\partial}{\partial j}(V^{*}v) + \alpha\beta hu\left(f + \frac{u\tan\theta}{a}\right) + g\alpha h\frac{\partial h}{\partial j} + R\alpha\beta hvq = \alpha\beta G .$$

Equation (4.15) is explicitly centered at the mesh point (i,j) for $2 \leq j \leq J-1$, as follows:

$$(4.17)\quad \frac{\partial}{\partial i}(U^*u) + \frac{\partial}{\partial j}(V^*u)$$

$$= \frac{1}{8}\{[(u_{i,j} + u_{i+1,j})(U^*_{i,j} + U^*_{i+1,j} + U^*_{i,j+1} + U^*_{i+1,j+1})$$

$$- (u_{i,j} + u_{i-1,j})(U^*_{i,j} + U^*_{i-1,j} + U^*_{i,j+1} + U^*_{i-1,j+1})]$$

$$+ [(u_{i,j} + u_{i,j+1})(V^*_{i,j} + V^*_{i+1,j} + V^*_{i,j+1} + V^*_{i+1,j+1})$$

$$- (u_{i,j} + u_{i,j-1})(V^*_{i,j} + V^*_{i+1,j} + V^*_{i,j-1} + V^*_{i+1,j-1})]\} ;$$

$$\alpha\beta hv(f + \frac{u \tan\theta}{a}) - R\alpha\beta huq + \alpha\beta F$$

$$\equiv \mathcal{H} v(f + \frac{u \tan\theta}{a}) - R\mathcal{H} uq + \alpha\beta F$$

$$= \frac{1}{4}(\mathcal{H}_{i,j} + \mathcal{H}_{i+1,j} + \mathcal{H}_{i,j+1} + \mathcal{H}_{i+1,j+1})$$

$$\cdot \left[v_{i,j}(f + \frac{u_{i,j} \tan\theta_j}{a}) - Ru_{i,j}q_{i,j}\right] + \alpha\beta F_{i,j} ,$$

where α is evaluated at θ_j;

$$g\beta h \frac{\partial h}{\partial i} = \frac{g\beta}{4}(h_{i,j} + h_{i+1,j} + h_{i,j+1} + h_{i+1,j+1}) \cdot (\frac{\partial h}{\partial i})_{\text{average}} ,$$

where $(\frac{\partial h}{\partial i})_{\text{average}}$ is evaluated after smoothing as in (4.7) through the formulas,

$$\left(\frac{\partial h}{\partial i}\right)_{\text{average}} = \left(\frac{\partial h}{\partial i}\right)^{(N_j)} ,$$

$$(4.18) \quad \left(\frac{\partial h}{\partial i}\right)^{(0)}_{i,j} = \frac{1}{2}\left[(h_{i+1,j+1} - h_{i,j+1}) + (h_{i+1,j} - h_{i,j})\right] ,$$

$$\left(\frac{\partial h}{\partial i}\right)^{(k)}_{i,j} = \left(\frac{\partial h}{\partial i}\right)^{(k-1)}_{i,j}$$

$$+ \kappa_j\left[\left(\frac{\partial h}{\partial i}\right)^{(k-1)}_{i-1,j} - 2\left(\frac{\partial h}{\partial i}\right)^{(k-1)}_{i,j} + \left(\frac{\partial h}{\partial i}\right)^{(k-1)}_{i+1,j}\right] ,$$

$$1 \leq k \leq N_j .$$

The explicit centered formulas for equation (4.16) in the range $2 \leq j \leq J-1$ are obtained from (4.17) by interchanging the variables u and v in all the places of (4.17) for which the corresponding terms in equations (4.15) and (4.16) are so related, and by setting

$$(4.19) \quad g\alpha h \frac{\partial h}{\partial j} \equiv g \frac{\mathcal{H}}{\beta} \frac{\partial h}{\partial j} = \frac{g}{8\beta}\left(\mathcal{H}_{i,j} + \mathcal{H}_{i+1,j} + \mathcal{H}_{i,j+1} + \mathcal{H}_{i+1,j+1}\right)$$

$$\cdot \left[(h_{i,j+1} - h_{i,j}) + (h_{i+1,j+1} - h_{i+1,j})\right] .$$

The definition of the smoothing parameters κ_j and N_j is based on the formulas:

$$(4.20) \qquad N_j \equiv \left[\frac{\beta}{\alpha}\right] , \quad \kappa_j \equiv \frac{\frac{\beta}{\alpha} - 1}{8N_j} \quad \text{for} \quad N_j \neq 0 ,$$

where the notation [x] represents the largest integer less than or equal to x, and the latitude at which α is defined depends on the quantity that is being smoothed. That is, for equation (4.7),

since the quantity U^*_{ij} is being calculated, α is evaluated at the latitude $\theta_j - \frac{\Delta\theta}{2}$ for $2 \leq j \leq J$; while for equation (4.18), since the quantity $\frac{\partial h}{\partial i}$ is being calculated, α is evaluated at latitude θ_j.

Furthermore, on the line $j = J$, equations (4.17), (4.18), and (4.19) are used with the variables

$$(4.21) \qquad h_{i,J+1} \equiv h_{J+1} , \quad \mathcal{H}_{i,J+1} \equiv \mathcal{H}_{J+1} , \quad V^*_{i,J+1} = 0 , \qquad \text{for } 1 \leq i \leq I ;$$

The fluxes $U^*_{i,J+1}$ are defined by using (4.6) with $j \equiv J+1$ and with

$$(4.22) \qquad (u_{i,J+1})_{average} = u^{(N_{J+1})}_{i,J+1} .$$

Here the value $u^{(0)}_{iJ}$ is obtained by averaging across the pole; namely, with I an even number,

$$u^{(0)}_{iJ} = \frac{u_{iJ} - u_{i+\frac{I}{2},J}}{2} ,$$

while $u^{(k)}_{iJ}$ is defined by (4.7) with the parameters N_j and κ_j defined by (4.20) for α evaluated at θ_J. Analogous formulas are used for equations (4.17), (4.18), and (4.19) on the line $j = 1$.

By using (4.13) and (4.14) in this manner, predicted values of $\hat{\mathcal{H}}_{ij}$ and then $\hat{u}_{ij}$ and $\hat{v}_{ij}$ are computed at each location for the time $t + \Delta t$. The final corrected values are then obtained at $t + \Delta t$ by using these predicted values to approximate the derivative with respect to time at $t + \Delta t$ that appears in each of the equations:

$$\mathcal{H}^{t+\Delta t} = \mathcal{H}^{t} + \Delta t\left(\frac{\partial \hat{\mathcal{H}}}{\partial t}\right)^{t+\Delta t},$$

$$(4.23) \qquad (\mathcal{H}u)^{t+\Delta t} = (\mathcal{H}u)^{t} + \Delta t\left(\frac{\partial (\widehat{\mathcal{H}u})}{\partial t}\right)^{t+\Delta t},$$

$$(\mathcal{H}v)^{t+\Delta t} = (\mathcal{H}v)^{t} + \Delta t\left(\frac{\partial (\widehat{\mathcal{H}v})}{\partial t}\right)^{t+\Delta t}.$$

That is, the formulas that were used to compute the terms $\left(\frac{\partial \mathcal{H}}{\partial t}\right)^{t}$, $\frac{\partial (\mathcal{H}u)^{t}}{\partial t}$, $\frac{\partial (\mathcal{H}v)^{t}}{\partial t}$ appearing in equations (4.13) and (4.14), are now evaluated with the use of the quantities $\hat{\mathcal{H}}$, $\hat{h}$, $\hat{u}$, $\hat{v}$ at the time $t+\Delta t$. In [1] this use of a backward time difference is called the Matsuno time differencing scheme.

4b. Friction Coefficient

The Mintz-Arakawa type difference scheme is more dissipative than either the Lax-Wendroff type scheme described in Section 3 or the Kreiss-Oliger type scheme described in Section 5. Hence for the interval sizes $\Delta\lambda$, $\Delta\theta$ that were used, the friction coefficient R for the Mintz-Arakawa type scheme is smaller by a factor of about 10. In fig. 14 and fig. 15 are plots of the decay of the kinetic energy of the entire layer and of the maximum speed respectively, for the zonal flow of (2.7), with D = 8.5km, $Q = 10\ \frac{\mathrm{m}}{\mathrm{sec}}$, and for each of the values $R = 5\times 10^{-9}\ \frac{1}{\mathrm{cm}}$, $8\times 10^{-9}\ \frac{1}{\mathrm{cm}}$.

4c. Climatological Flow

The planar flow, that is described by using the function $\Phi(x,y)$ of (2.25), has the planar velocity components (μ,ν) and the height h given by

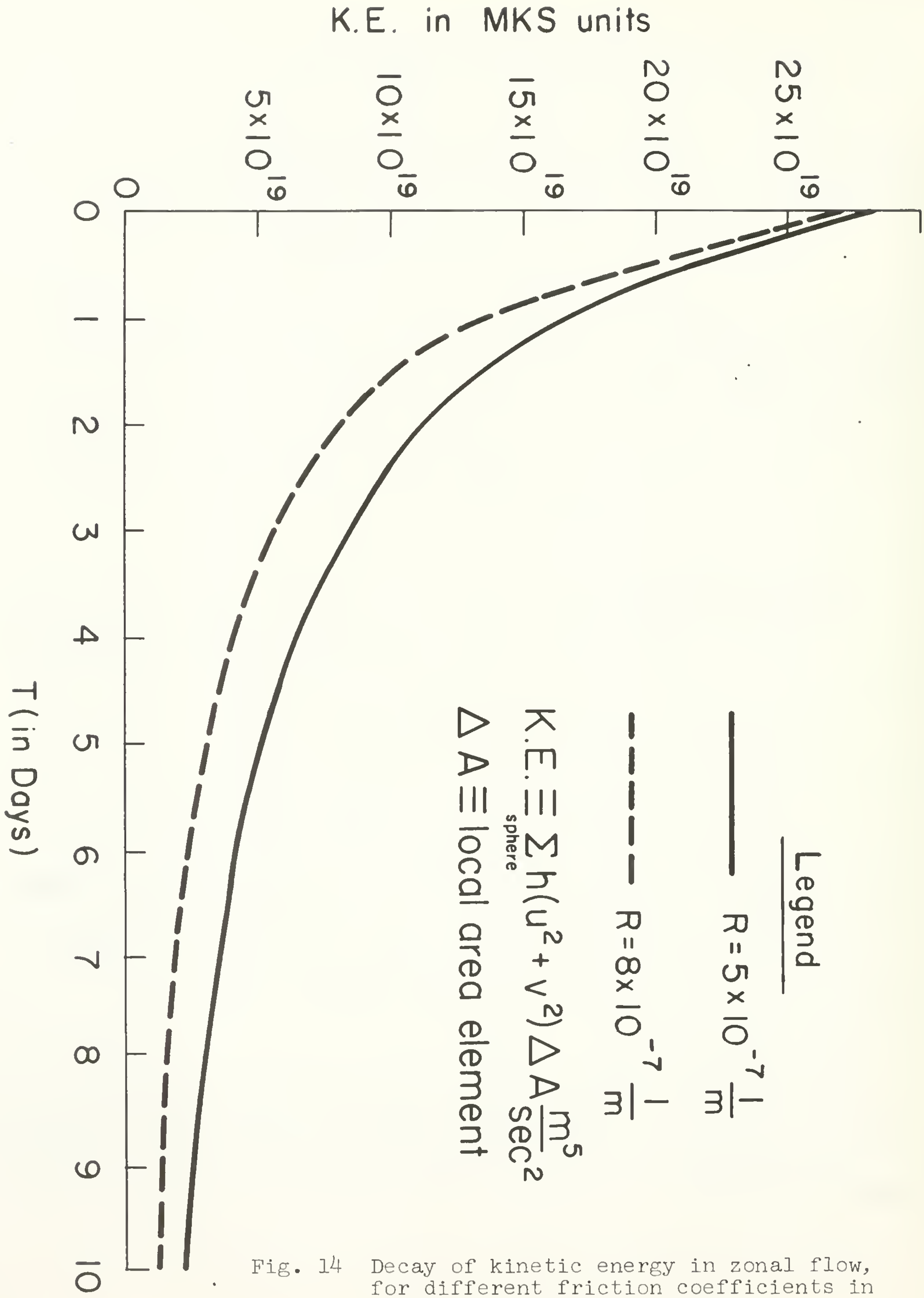

Fig. 14 Decay of kinetic energy in zonal flow, for different friction coefficients in the Mintz-Arakawa type scheme.

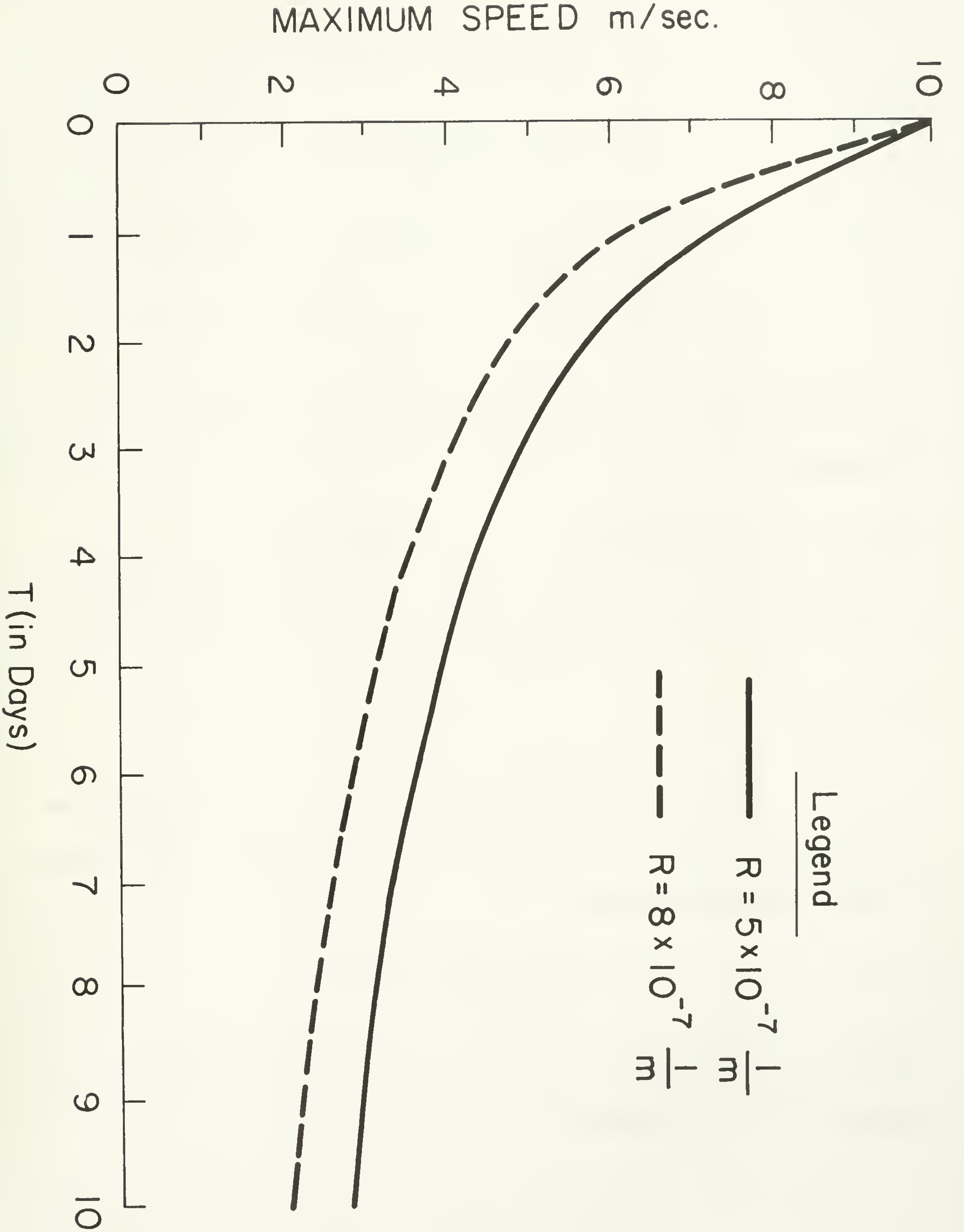

Fig. 15 Decay of maximum speed in zonal flow for different friction coefficients in the Mintz-Arakawa type scheme.

$$\mu = -\Phi_y \; ,$$

(4.24) $$\nu = \Phi_x \; ,$$

$$h = D + \frac{f}{g}\Phi \, ,$$

where

$$\Phi = -\frac{1}{2\pi}\sum_{i=0}^{3} \gamma_i \hat{K}_o(\kappa\rho_i) \; ,$$

and

$$\rho_i^2 = (x - x_i)^2 + (y - y_i)^2 \; .$$

The height distribution could be transferred to the sphere through the mapping

(4.25) $$x = a(\frac{\pi}{2} - \theta)\cos\lambda \; , \qquad y = a(\frac{\pi}{2} - \theta)\sin\lambda$$

and the spherical velocity components (u, v) could be defined by

(4.26) $$\begin{cases} u \equiv -\mu \sin\lambda + \nu \cos\lambda \\ v = -\mu \cos\lambda - \nu \sin\lambda \; . \end{cases}$$

In order to simplify subsequent calculations, the formulas for the climatological flow $\tilde{h}$, $\tilde{u}$, $\tilde{v}$ were defined on the sphere as follows for the northern hemisphere:

(4.27) $$\tilde{h} = D - \frac{f}{2\pi g}\sum_{i=0}^{3} \gamma_i \hat{K}_o(\kappa\tilde{\rho}_i) \; ,$$

$(\tilde{u}, \tilde{v})$ are determined from (4.26) with the quantities μ and ν replaced by $\tilde{\mu}$ and $\tilde{\nu}$ respectively, where

$$\tilde{\mu} = \frac{1}{2\pi}\sum_{i=0}^{3} \gamma_i \kappa \hat{K}_o'(\kappa\tilde{\rho}_i) \cdot \frac{y - y_i}{\tilde{\rho}_i} ,$$

(4.28)

$$\tilde{\nu} = -\frac{1}{2\pi}\sum_{i=0}^{3} \gamma_i \kappa \hat{K}_o'(\kappa\tilde{\rho}_i) \cdot \frac{x - x_i}{\tilde{\rho}_i} .$$

Here the variables (x,y) and (x_i,y_i) are now expressed in terms of (λ,θ) and (λ_i,θ_i) by using (4.25) and the formula for $\tilde{\rho}_i$ is the spherical distance between this pair of points:

(4.29) $$\tilde{\rho}_i \equiv a\phi_i$$

where

$$\cos \phi_i = \sin \theta \sin \theta_i + \cos \theta \cos \theta_i \cos (\lambda - \lambda_i) .$$

Note that the spherical velocity field $(\tilde{u},\tilde{v})$ that is hereby defined does not correspond to the usual transformation of the planar velocity field (μ,ν) under the mapping (4.25). That is,

$$\begin{cases} \tilde{u} \neq \frac{d}{dt} \lambda(x,y) , \\ \tilde{v} \neq \frac{d}{dt} \theta(x,y) \end{cases}$$

where $(x(t),y(t))$ represents a particle path in the planar flow defined by (4.24). Nevertheless, the quantities $(\tilde{u},\tilde{v})$ may now be considered to represent a velocity field in the northern hemisphere. The essential cyclonic or anti-cyclonic character of a planar low or high is preserved. The flow is then defined in the southern hemisphere, by requiring symmetry across the equator.

Upon prescribing $[\lambda_i(t),\theta_i(t)]$, the position of the centers of the subtropical highs and the polar low, the climatological flow $\tilde{h}$, $\tilde{u}$, $\tilde{v}$ is defined as a function of time.

Now, if the differential operators appearing in equations (4.1), (4.2), and (2.3) are thought of respectively as

$$\mathcal{L}_1(u,v,h) = 0 \ ,$$

$$\mathcal{L}_2(u,v,h) = 0 \ ,$$

$$\mathcal{L}_3(u,v,h) = 0 \ ,$$

then the forced system

$$\mathcal{L}_1(u,v,h) = F \ ,$$

$$\mathcal{L}_2(u,v,h) = G \ , \tag{4.30}$$

$$\mathcal{L}_3(u,v,h) = Q$$

is solved by the difference scheme defined in Section 4a. For the choice,

$$F \equiv \mathcal{L}_1(\tilde{u},\tilde{v},\tilde{h}) \ ,$$

$$G \equiv \mathcal{L}_2(\tilde{u},\tilde{v},\tilde{h}) \ ,$$

$$Q \equiv \mathcal{L}_3(\tilde{u},\tilde{v},\tilde{h}) \ ,$$

the system (4.30) can be represented as

$$\mathcal{L}(u,v,h) = \mathcal{L}(\tilde{u},\tilde{v},\tilde{h}) \ . \tag{4.31}$$

Again, the right-hand sides are defined in the southern hemisphere by symmetry across the equator, e.g. $\tilde{v} = 0$ on the equator. Hence, if at time $t = 0$ the initial data are given by

$$(u,v,h) = (\tilde{u},\tilde{v},\tilde{h}) \ , \tag{4.32}$$

then the equation (4.32) will represent the solution of (4.31) for all time.

On the other hand, the difference scheme defined in Section 4a may be thought of as defining the functions $(u_\Delta, v_\Delta, h_\Delta)$ that satisfy the initial condition (4.32) and the difference equation system (on the mesh Δ)

$$\mathcal{L}_\Delta(u_\Delta, v_\Delta, h_\Delta) = \mathcal{L}(\tilde{u}, \tilde{v}, \tilde{h}) \ . \tag{4.33}$$

Hence, the errors $u_\Delta - u$, $v_\Delta - v$, and $h_\Delta - h$ may be determined by simply subtracting the known solution of (4.31), (4.32) from the computed values $(u_\Delta, v_\Delta, h_\Delta)$, found in the difference scheme.

A plot of the contours of the initial height field $\tilde{h}$ is drawn in fig. 16 for a symmetrical climatological flow with parameter values

$$D = 8{,}429.6\text{m} \ ,$$

$$\gamma_0 = 3.26 \times 10^7 \ ,$$

$$\gamma_1 = \gamma_2 = \gamma_3 = -4.0 \times 10^8 \ ,$$

$$\kappa = 5.886 \times 10^{-7} \ ,$$

$$\theta_i(0) = \frac{\pi}{6} \ , \quad i = 1,2,3,$$

with the function $\hat{K}_0$ defined as in the first graph of fig. 1, for $x_1 = 1.762$. The contours are plotted at an interval of 30.28 meters, with the maximum value of $h \equiv M = 8726.9$m, attained at the centers of the highs, and the minimum value of $h \equiv m = 8424.2$m, attained at the poles. With this choice of $\tilde{h}$, $\tilde{u}$, $\tilde{v}$ held steady in time, the computed solution h_Δ, u_Δ, v_Δ was found to tend to a

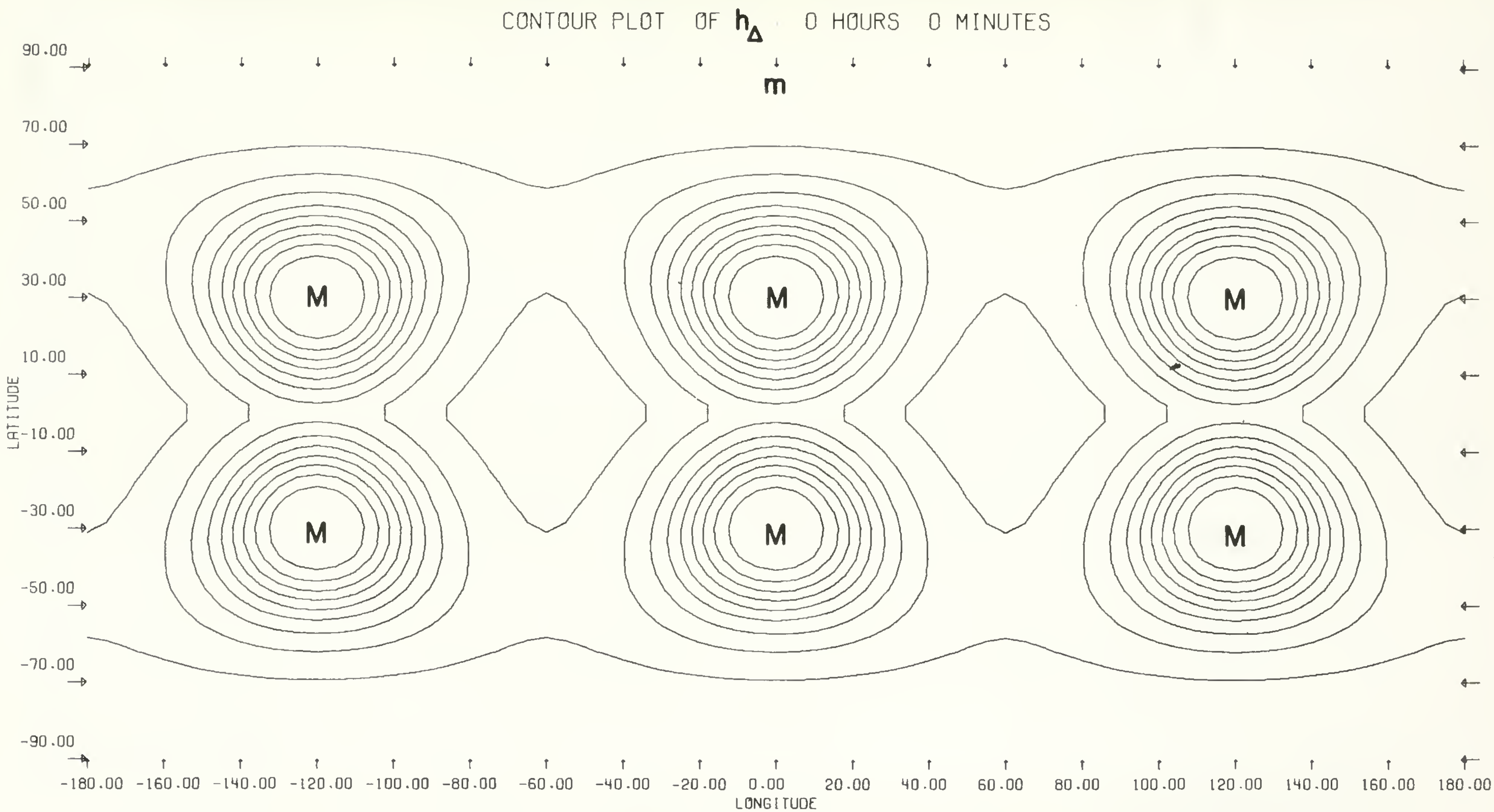

Fig. 16 Contours of the initial height field $\tilde{h}$, plotted in (λ, θ) coordinates. Maximum value of $\tilde{h}$ = 8726.9m = **M**; minimum value of $\tilde{h}$ = 8424.2m = **m**; contour interval = 30.28m. The highs are centered at $\pm 30^{\circ}$ latitude and are 120° apart. The lows are centered at the poles.

steady state within about 48 hours. In fig. 17, the contours of h_Δ are plotted at time $t = 48$ hours at the intervals that are used in fig. 16. Notice that there are eleven contour lines at $t = 48$ hours, in each hemisphere, whereas there were only nine at $t = 0$ hours. One of the two new contour levels corresponds to the maximum value of h at $t = 0$, which appears since the small truncation errors produce an increase in the maximum value of h_Δ as time increases. The additional closed contour lines that appear along the equator are evidence of slight elevations, which also arise from the truncation error of the scheme.

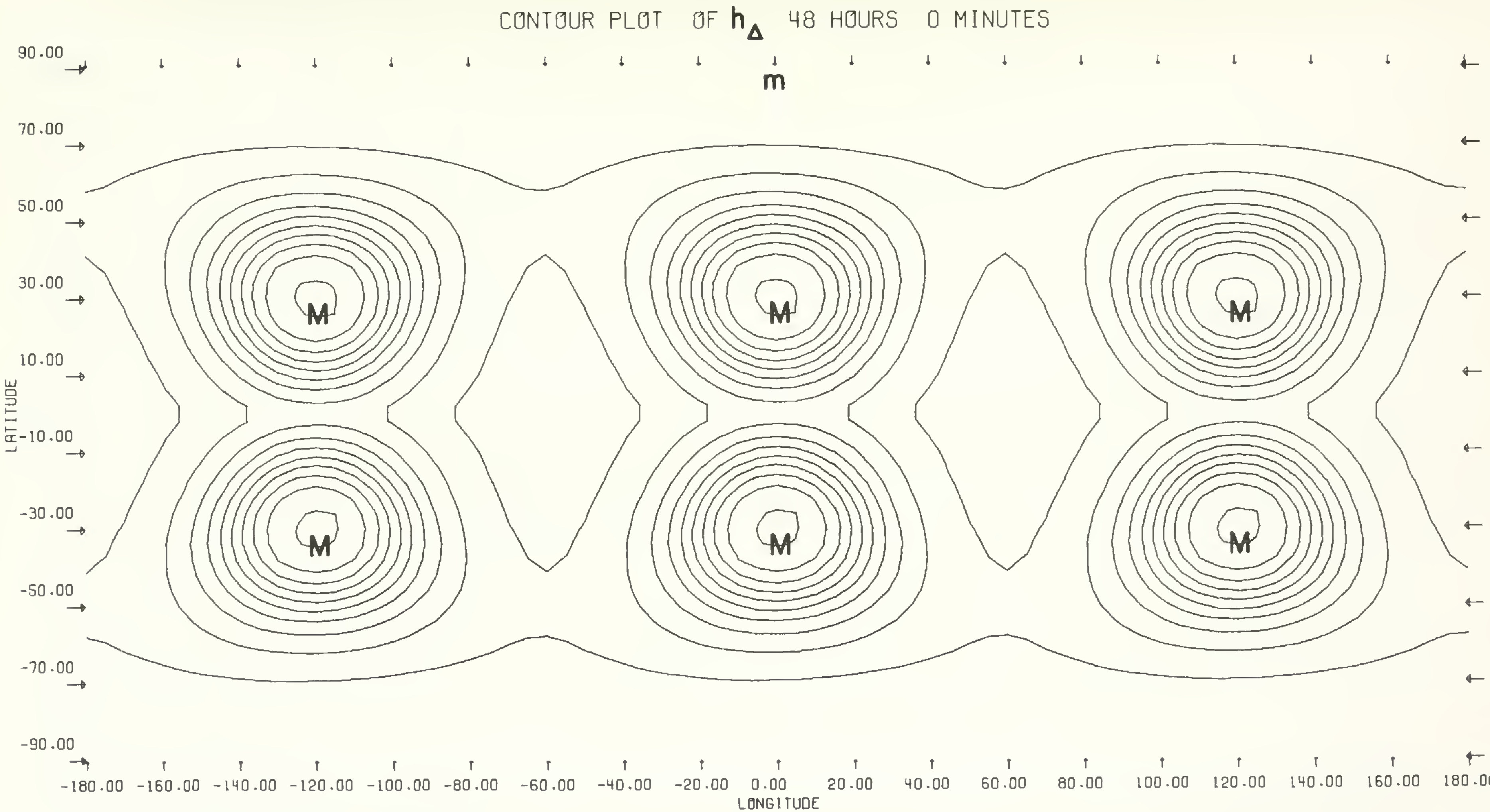

Fig. 17 Contours of the height field h_Δ, plotted at $t = 48$ hours. The contour levels are the same as those used in Fig. 16. The level $h_\Delta = M$ appears innermost at the highs. The small closed contours at the equator correspond to 8454.5m as do their nearest open lines.

5. The Kreiss-Oliger Scheme

5a. Difference Scheme

A leap-frog, explicit scheme, that is accurate to second order in the time increment and to fourth order in the space increment, had been devised and used for the system (2.1)-(2.3) by Kreiss and Oliger [6], with R = 0. The variables (u,v,h) are computed on a uniform grid in (λ, θ) coordinates. Hence, to avoid the necessity of using a small time step Δt, Williamson and Browning [13] implemented this scheme by incorporating the fast Fourier transform technique to smooth the computed values of (u,v,h) at $t + \Delta t$, on lines of latitude near the poles. They were kind enough to make their program available. Subsequently, modifications were made here to deal with the case of forced motion and friction, i.e. $R \neq 0$. The details of the scheme will now be sketched.

The fast Fourier transform algorithm is most efficient when it uses a power of 2 for the number I of net points on a line of latitude. Therefore, the choices $\Delta\theta = \frac{2\pi}{64}$ corresponding to $I = 2^6$, and $\Delta\lambda = \frac{\pi}{32}$ were made. Let ψ^n_{ij} denote a quantity ψ defined at the mesh point (λ_i, θ_j) at the time t_n. The generic partial derivative expressions $(\frac{\partial\psi}{\partial t}, \frac{\partial\psi}{\partial\lambda}, \frac{\partial\psi}{\partial\theta})$ appearing in equations (2.1)-(2.3) are replaced by the following generic centered difference formulas:

$$\frac{\partial\psi}{\partial t} \cong \delta_t\psi^* \equiv \frac{\psi^{*n+1} - \psi^{n-1}}{2\Delta t} \tag{5.1*}$$

$$(5.2) \qquad \frac{\partial\psi}{\partial\lambda} \cong \delta_\lambda\psi \equiv \frac{4}{3}\left[\frac{\psi_{i+1,j} - \psi_{i-1,j}}{2\Delta\lambda}\right] - \frac{1}{3}\left[\frac{\psi_{i+2,j} - \psi_{i-2,j}}{4\Delta\lambda}\right] ,$$

$$(5.3) \qquad \frac{\partial\psi}{\partial\theta} \cong \delta_\theta\psi \equiv \frac{4}{3}\left[\frac{\psi_{i,j+1} - \psi_{i,j-1}}{2\Delta\theta}\right] - \frac{1}{3}\left[\frac{\psi_{i,j+2} - \psi_{i,j-2}}{4\Delta\theta}\right] .$$

Here ψ^{*n+1} represents the predicted value of ψ at time step (n+1). Later, a formula for the corrected value ψ^{n+1} at time step (n+1) will be given. The coefficients of the differentiated quantities in equations (2.1)-(2.3) are evaluated at $(\lambda_i, \theta_j, t_n)$. The Coriolis terms in equations (2.1) and (2.2) are replaced respectively by

$$(5.4^*) \qquad (f + \frac{u}{a} \tan\theta)\overline{v}^* , \qquad (f + \frac{u}{a} \tan\theta)\overline{u}^* ,$$

where

$$(5.5^*) \qquad \overline{v}^* \equiv \frac{v^{*n+1} + v^{n-1}}{2} , \qquad \overline{u}^* \equiv \frac{u^{*n+1} + u^{n-1}}{2} .$$

The friction terms in equations (2.1) and (2.2) are replaced respectively by

$$(5.6^*) \qquad R\overline{u}^* q^n , \qquad R\overline{v}^* q^n ,$$

with the average values $\overline{u}^*$, $\overline{v}^*$ defined in (5.5*). In case the right-hand sides of equations (2.1)-(2.3) are non-zero, say (E,F,G) respectively, then these expressions are evaluated at $(\lambda_i, \theta_j, t_n)$. Under the difference prescriptions (5.1*), (5.2), (5.3), (5.4*)-(5.6*), the unknown predicted values u^{*n+1}, v^{*n+1}, h^{*n+1} appear linearly in a set of three simultaneous equations with coefficients that depend on quantities defined at the two previous times t_n

and t_{n-1}. Explicit formulas can thus be derived for u^{*n+1}, v^{*n+1}, h^{*n+1} at each net point (i,j), provided that special attention is given to the case that (i,j) is near a pole.

To avoid the situation that (i,j) is at a pole, the values θ_j were defined as in the code of Williamson and Browning by

$$(5.7) \qquad \theta_j \equiv -\frac{\pi}{2} + (j - \frac{1}{2})\Delta\theta \quad \text{for} \quad 1 \leq j \leq 32 .$$

Hence

$$-\frac{\pi}{2} + \frac{\Delta\theta}{2} \leq \theta_j \leq \frac{\pi}{2} - \frac{\Delta\theta}{2} ,$$

and (i,j) does not lie at a pole. It is also apparent that (i,j) does not lie on the equator either. When at (λ_i, θ_j) the value $j = 1, 2, 31,$ or 32, then one or two points that appear in the difference expression δ_θ will straddle the pole on the same great circle of longitude. In such cases, the values of u and v that lie on the other side of the pole are replaced by -u and -v respectively in (5.3). To prevent the separation of the solution between the even and odd numbered time steps, that is characteristic of leap-frog schemes, a corrector step is used to define $(u^{n+1}, v^{n+1}, h^{n+1})$ explicitly. That is, equation (5.1*) is modified as

$$(5.1) \qquad \frac{\partial\psi}{\partial t} \cong \delta_t\psi \equiv \frac{\psi^{n+1} - \psi^{n-1}}{2\Delta t} ;$$

the Coriolis expressions (5.4*) and (5.5*) are modified as

$$(5.4) \qquad (f + \frac{u}{a} \tan\theta)\overline{v} , \quad (f + \frac{u}{a} \tan\theta)\overline{u} ,$$

where

$$(5.5) \qquad \bar{v} = \frac{v^{n+1} + v^{n-1}}{2} , \qquad \bar{u} = \frac{u^{n+1} + u^{n-1}}{2} ;$$

finally the friction terms (5.6*) are modified by using the predicted speed q^{*n+1}

$$(5.6) \qquad R\bar{u}\,\frac{q^{*n+1} + q^{n-1}}{2} , \qquad R\bar{v}\,\frac{q^{*n+1} + q^{n-1}}{2} .$$

Smoothing of the values $(u^{n+1}, v^{n+1}, h^{n+1})$, on several lines of latitude nearest the poles, is now performed by the use of the fast Fourier transform. This avoids the use of a time step Δt that is proportional to the arclength of the shortest mesh interval, i.e.

$$a\Delta\lambda \cos\left(\frac{\pi}{2} - \frac{\Delta\theta}{2}\right) \cong \frac{a}{2}\,\Delta\lambda\Delta\theta .$$

The fast Fourier transform algorithm determines the coefficients c_k of the finite Fourier series, $\phi(\lambda)$, that interpolates the 2π periodic function $\psi(\lambda)$ at the points

$$\lambda_p = p\left(\frac{2\pi}{I}\right) , \qquad 0 \leq p \leq I = 64 ,$$

in the complex form:

$$(5.8) \qquad \phi(\lambda) = \sum_{k=0}^{I-1} c_k e^{ik\lambda} .$$

That is,

$$\phi(\lambda_p) = \psi(\lambda_p) , \qquad 0 \leq p \leq I ,$$

and the coefficients c_k are uniquely determined by the sum:

(5.9) $$c_k = \frac{1}{I}\sum_{k=0}^{I-1} \psi(\lambda_p)e^{-ik\lambda_p}\,, \quad 0 \le k \le I-1\,.$$

Observe that when $\psi(\lambda)$ is real, then

$$c_{I-k} = \bar{c}_k\,, \quad 0 \le k \le I-1\,.$$

Hence, $\phi(\lambda)$ may be written as a real finite Fourier series in the form

(5.10) $$\phi(\lambda) = \sum_{k=0}^{I/2} a_k \cos k\lambda + b_k \sin k\lambda\,,$$

with

$$a_k = 2\,\mathrm{Re}\,c_k\,, \quad b_k = 2\,\mathrm{Im}\,c_k\,, \quad 1 \le k < \frac{I}{2}\,;$$

$$a_o = c_o\,, \quad b_o = 0\,; \quad a_{I/2} = c_{I/2}\,, \quad b_{I/2} = 0\,.$$

When the longitudinal variable λ is used on a line of latitude θ, then the wavelength $\frac{2\pi}{k}$, of the terms $\cos k\lambda$ and $\sin k\lambda$, has the arclength s, where

$$s = \frac{2\pi}{k}\, a \cos\theta\,.$$

Hence, the smoothing of $\psi(\lambda)$ may be obtained by eliminating those terms in (5.10) for which the arclength s is less than $\frac{a\Delta\theta}{2}$. That is, $\psi(\lambda)$ is approximated by the function $\zeta(\lambda)$, where

(5.11) $$\zeta(\lambda) = \sum_{k=0}^{q} a_k' \cos k\lambda + b_k' \cos k\lambda\,,$$

with

$$q = q(\theta) \equiv \min\left(\frac{4\pi\cos\theta}{\Delta\theta}, \frac{I}{2}\right)$$

$$= \min\,(64\cos\theta,\ 32)\,.$$

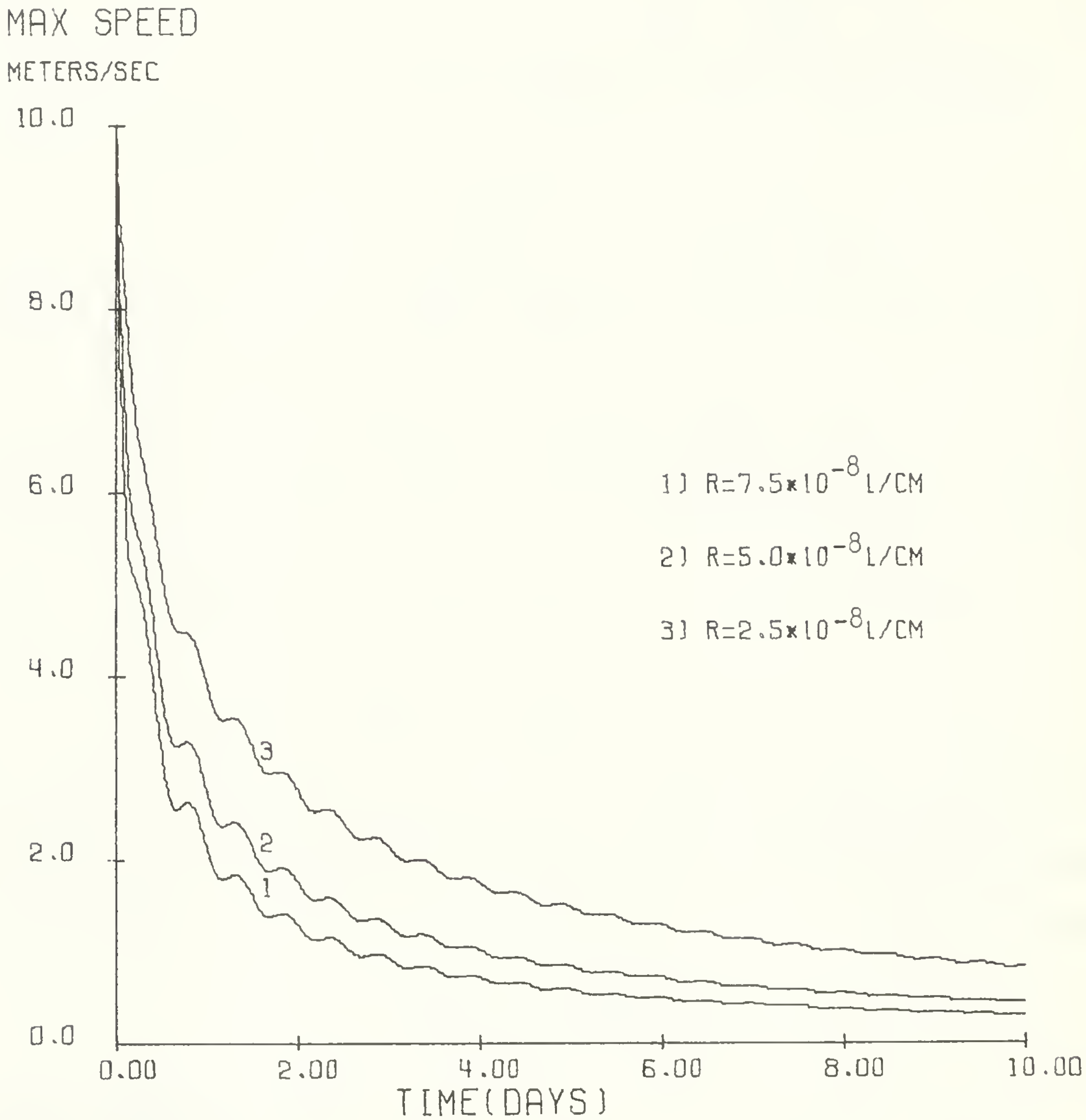

Fig. 18 Decay of maximum wind speed in a zonal flow, for three values of the friction coefficient R.

Here, if $q = \frac{I}{2} = 32$, then $a_k' \equiv a_k$, and $b_k' \equiv b_k$ for $0 \leq k \leq q$. But, if $q < 32$, then

$$a_k' \equiv a_k \;, \quad b_k' \equiv b_k \quad \text{for} \quad 0 \leq k \leq q-2 \;;$$

while for the last two coefficients

$$\begin{aligned} a_{q-1}' &\equiv .75a_{q-1} \;, \quad & b_{q-1}' &\equiv .75b_{q-1} \;, \\ a_q' &\equiv .25a_q \;, \quad & b_q' &\equiv .25a_q \;. \end{aligned} \tag{5.12}$$

For the case $I = 64$, the values of $q(\theta)$ were 3, 9, 15, 21, 27 on the five lines of latitude nearest to each pole. Hence $(u^{n+1}, v^{n+1}, h^{n+1})$ are smoothed by truncating the trigonometric interpolation formula and decreasing the last coefficients.

An interval size $\Delta t = 360$ sec was used to insure stability of the scheme for the cases we treated.

5b. Friction Coefficient, Spin-down Time

The Kreiss-Oliger scheme is less dissipative than either of the other two schemes. In fig. 18, are plots of the decay of the maximum speed, that occur when the initial state is the zonal flow (2.7) with $D = 8.5$km, $Q = 10\ \frac{m}{sec}$. Three different values of the friction coefficient are used: $R = 7.5 \times 10^{-8}\ \frac{1}{cm}$, $5.0 \times 10^{-8}\ \frac{1}{cm}$, $2.5 \times 10^{-8}\ \frac{1}{cm}$.

5c. Climatological Flow

Figure 19 shows, in stereographic plane, the contour lines of the initial height $\tilde{h}$ of the layer, for the climatological flow with

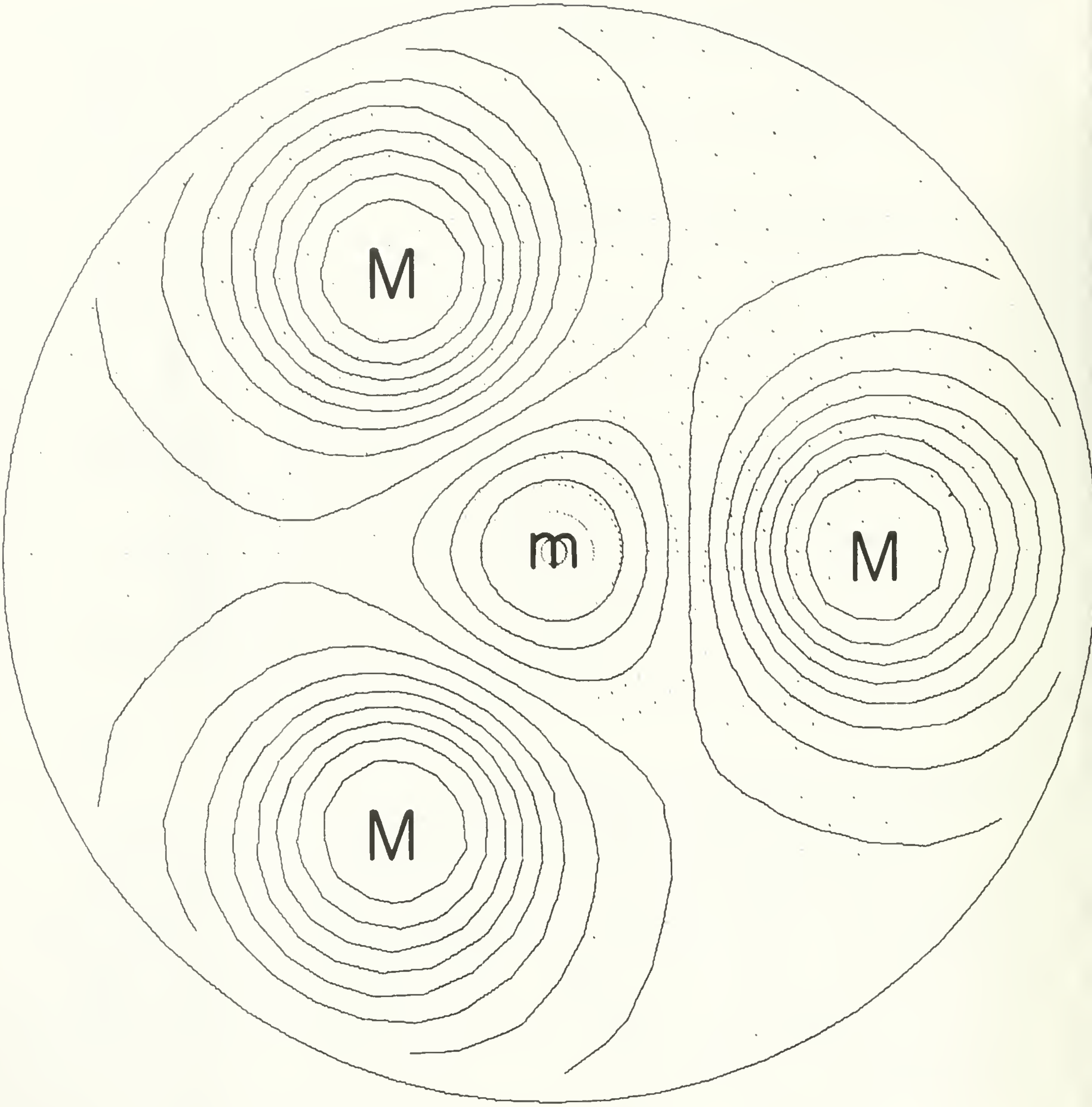

Fig. 19 Contour lines of the initial height $\tilde{h}$. The maximum level line corresponds to $\tilde{h} = 8.66 \times 10^5$cm. The minimum level line corresponds to $\tilde{h} = 8.46 \times 10^5$cm. The contour interval is $.02 \times 10^5$cm. The letter **M** appears where $\tilde{h} \cong 8.67 \times 10^5$cm; the letter **m** appears where $\tilde{h} \cong 8.44 \times 10^5$cm.

three subtropical highs at 30° latitude and a polar low, as given by equation (4.27). The mesh points used in the scheme are indicated by light dots. The value

$$\gamma_o = -0.419\gamma_i \ , \quad i = 1,2,3$$

was used to ensure that the initial velocity at the centers of the highs is zero. The other parameters in (4.27) were defined in c.g.s. units as: $\gamma_i = -4.5 \times 10^{12} (\mathrm{cm})^2$ for $i = 1,2,3$; $D = 8.5 \times 10^5 \mathrm{cm}$. The function $\hat{K}_o$ was chosen as in Section 4 (see fig. 1 for $x_1 = 1.762$), with $\kappa\rho_i = 3.75$, where ρ_i is the spherical distance from the pole to latitude 30°. The Coriolis parameter in (4.27) is evaluated at the pole. The corresponding climatological velocity components $\tilde{u}$ and $\tilde{v}$ are then defined (as in Section 4).

Equations (2.1)-(2.3) may be written respectively in the form

$$\mathcal{L}_1(u,v,h) = 0 \ ,$$

$$\mathcal{L}_2(u,v,h) = 0 \ ,$$

$$\mathcal{L}_3(u,v,h) = 0 \ .$$

The forced system

$$\begin{aligned} \mathcal{L}_1(u,v,h) &= \mathcal{L}_1(\tilde{u},\tilde{v},\tilde{h}) \equiv E \ , \\ \mathcal{L}_2(u,v,h) &= \mathcal{L}_2(\tilde{u},\tilde{v},\tilde{h}) \equiv F \ , \qquad (5.13) \\ \mathcal{L}_3(u,v,h) &= \mathcal{L}_3(\tilde{u},\tilde{v},\tilde{h}) \equiv G \ , \end{aligned}$$

with initial condition

$$(u,v,h)\Big|_{t=0} = (\tilde{u},\tilde{v},\tilde{h})\Big|_{t=0}$$

has the unique solution

$$(u,v,h) = (\tilde{u},\tilde{v},\tilde{h}) \text{ .}$$

Note that system (5.13) corresponds to the velocity form of the equations of motion, while equations (4.30) and (4.31) corresponded to the momentum form of the equations of motion. The case that $(\tilde{u},\tilde{v},\tilde{h})$ is independent of time was treated.

Figure 20 shows the contour lines of the approximate solution h_Δ of the system (5.13) at time t = 2 days, as obtained by the predictor-corrector method of Kreiss-Oliger. The solution $(u_\Delta, v_\Delta, h_\Delta)$ has become steady.

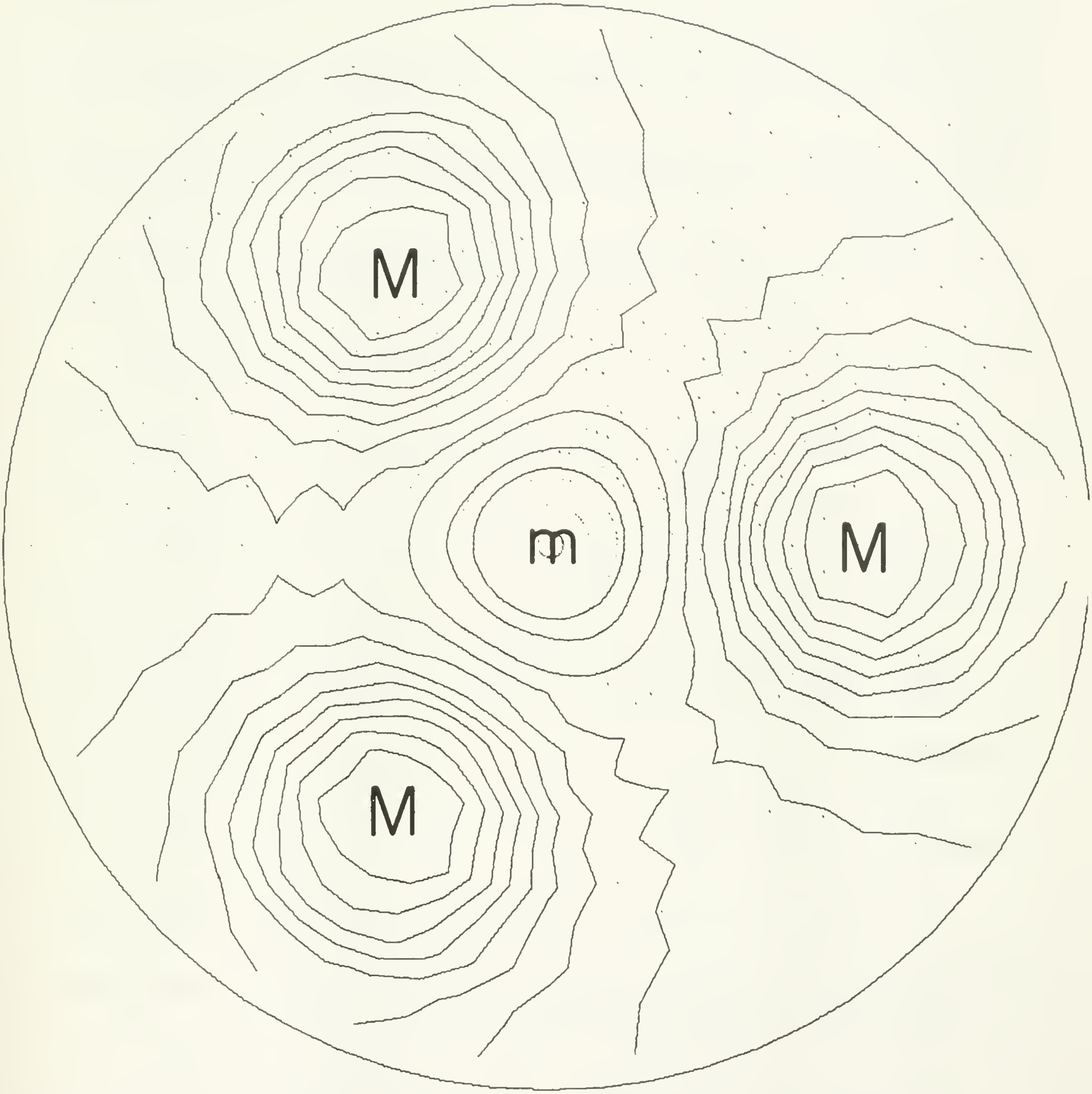

Fig. 20 Contour lines of the height h_{Δ} after two days, produced by the Kreiss-Oliger scheme. The contour levels are the same as appear in Fig. 19.

6. Summary and Publications

The three numerical schemes have been used to compute non-steady motions for periods of ten to twenty days. The Mintz-Arakawa and the Kreiss-Oliger type methods conserve the total mass of the atmosphere adequately. But, the stereographic coordinate scheme ultimately gains mass at a small constant rate, after the first day. Therefore, the stereographic coordinate scheme must be improved before it can be used for long term integration. The time step required by this scheme is approximately twice as large as for the other schemes. A method has been formulated for modifying a difference scheme so as to force the "exact" conservation of total mass, energy, vorticity, etc. This work is not well enough advanced to permit evaluation.

Hopefully long term integrations may then be performed with all three schemes, in order (a) to decide upon the accuracy of the average values of such computed solutions, and (b) to determine which type of scheme may be the most economical for application to other models.

The following list of reports, papers, and theses was prepared under ARPA sponsorship. The thesis of M. Ghil is concerned with establishing the stability and instability of the steady state solutions of the Schneider, Gal-Chen energy balance climate model.

The thesis of A. Bayliss studies the asymptotic behavior for $t \to \infty$ of the solution of a forced system of ordinary difference equations. The forcing function is almost periodic in the time. The difference equations result from approximating the solution of certain differential equations.

List of publications prepared under ARPA grant

Bauer, L. and G.K. Morikawa, "Stability of rectilinear geostrophic vortices in stationary equilibrium", Report no. IMM-406, CIMS-NYU, to appear Apr. 1975.

Bayliss, Alvin, "Exponential dichotomies and almost periodic solutions to difference equations", PhD thesis in preparation, NYU, 1975.

Drew, D.A., "The zonally symmetric motion of the atmosphere", Report no. IMM-401, CIMS-NYU, Aug. 1973.

Friedlander, Susan, "Spin-down in a rotating fluid; part I", Studies in App. Math., MIT, vol. 53, no. 2, pp. 111-136, 1974.

Friedlander, Susan, "Interaction of vortices in a fluid on the surface of a rotating sphere", paper accepted by Tellus, 1974.

Ghil, Michael, "Numerical methods in fluid mechanics", paper to appear in Proc. 1973 summer school of Les Houches, France.

Ghil, Michael, "On balance and initialization", Report no. IMM-400, CIMS-NYU, Dec. 1973, accepted by J. Atm. Sciences.

Ghil, Michael, "A nonlinear parabolic equation with applications to climate theory", PhD thesis in preparation, NYU, 1975.

Leiva, C., "Stability of geostrophic vortices on a sphere", Report no. IMM-405, CIMS-NYU, Dec. 1974.

Peters, A.S., "Motion of a vortex in a rotating layer of fluid between rigid concentric spheres", Report no. IMM-398, CIMS-NYU, Sept. 1973.

Peters, A.S., "Geostrophic vortices on a sphere", Report no. IMM-399, CIMS-NYU, Oct. 1973.

Peters, A.S., "Geostrophic vortices on a circle of latitude in a cap on a rotating sphere", Report no. IMM-404, CIMS-NYU, July 1974.

Stoker, J.J., "Numerical solution of two problems in geophysics", Acad. Nat'l dei Lincei, Rome, Italy.

7. Bibliography

1. Arakawa, A., "Design of the UCLA general circulation model", Tech. Report No. 7, July 1972, Dept. of Meteorology, Univ. of Cal. at Los Angeles, Los Angeles, Ca. 90024.

2. Bauer, L., and G. K. Morikawa, "Stability of rectilinear geostrophic vortices in stationary equilibrium", Report No. IMM-406, CIMS-NYU, to appear Apr. 1975.

3. Gary, J. M., "A comparison of two difference schemes used for numerical weather prediction", J. Comput. Phys., Vol. 4, 1969, pp. 279-305.

4. Gates, W. L., E. S. Batten, A. B. Kahle and A. B. Nelson, "A documentation of the Mintz-Arakawa two-level atmospheric general circulation model", Report No. R-877-ARPA, Dec. 1971, Rand Corp., Santa Monica, Ca. 90406.

5. Grimmer, M., and D. B. Shaw, "Energy-preserving integration of the primitive equations on the sphere", Quart. J. Roy. Meteor. Soc., Vol. 93, No. 397, July 1967, pp. 337-349.

6. Kreiss, H.-O., and J. Oliger, "Comparison of accurate methods for the integration of hyperbolic equations", Tellus, Vol. 24, 1972, pp. 199-215.

7. Mintz, Y., "Very long-term global integration of the primitive equations of atmospheric motion", in WMO Tech. Note No. 66, 1965, pp. 141-167.

8. Morikawa, G. K., "Geostrophic vortex motion", J. Meteorol., Vol. 17, 1960, pp. 148-158.

9. Morikawa, G. K., and E. V. Swenson, "Interacting motion of rectilinear geostrophic vortices", Phys. Fluids, Vol. 14, 1971, pp. 1058-1073.

10. Warshaw, M., and R. R. Rapp, "An experiment on the sensitivity of a global circulation model: Studies in climate dynamics for environmental security", Report No. R-908-ARPA, Feb. 1972, Rand Corp., Santa Monica, Ca. 90406.

11. Stewart, H. J., "Periodic properties of the semi-permanent atmospheric pressure systems", Quart. Appl. Math., Vol. 1, 1943, pp. 262-267.

12. Umscheid, L., Jr., and M. Sankar-Rao, "Further tests of a grid system for global numerical prediction", Mon. Wea. Rev., Vol. 99, No. 9, Nov. 1971, pp. 686-690.

13. Williamson, D. L., and G. L. Browning, "Comparison of grids and difference approximations for numerical weather prediction over a sphere", J. Appl. Meteor., Vol. 9, 1970, pp. 262-274.

8. Acknowledgment

The extensive numerical experimentation would not have been possible without the generous and able assistance of the ERDA Mathematics and Computing Laboratory operated under Contract No. AT(11-1)-3077.

REPORT DOCUMENTATION PAGE

READ INSTRUCTIONS BEFORE COMPLETING FORM

1. REPORT NUMBER: IMM 407	2. GOVT ACCESSION NO.
3. RECIPIENT'S CATALOG NUMBER	
4. TITLE (and Subtitle): Final Report, I	5. TYPE OF REPORT & PERIOD COVERED: Final Report, I 2/15/72 - 5/31/73, (cont)
	6. PERFORMING ORG. REPORT NUMBER
7. AUTHOR(s): J. J. Stoker and E. Isaacson	8. CONTRACT OR GRANT NUMBER(s): DA-ARO-D-31-124-72-G113, DA-ARO-D-31-124-73-G150, AFOSR-74-2728.
9. PERFORMING ORGANIZATION NAME AND ADDRESS: Courant Institute of Mathematical Sciences, New York University, 251 Mercer Street, New York, N.Y. 10012	10. PROGRAM ELEMENT, PROJECT, TASK AREA & WORK UNIT NUMBERS: ARPA Order 2774
11. CONTROLLING OFFICE NAME AND ADDRESS: Advanced Research Projects Agency, 1400 Wilson Boulevard, Arlington, Virginia 22209	12. REPORT DATE: January 1975
	13. NUMBER OF PAGES: 75
14. MONITORING AGENCY NAME & ADDRESS (if different from Controlling Office): Air Force Office of Scientific Research, 1400 Wilson Boulevard, Arlington, Virginia 22209	15. SECURITY CLASS. (of this report): none
	15a. DECLASSIFICATION/DOWNGRADING SCHEDULE

16. DISTRIBUTION STATEMENT (of this Report)

Distribution of this document is unlimited.

17. DISTRIBUTION STATEMENT (of the abstract entered in Block 20, if different from Report)

none

18. SUPPLEMENTARY NOTES

none

19. KEY WORDS (Continue on reverse side if necessary and identify by block number)

climate dynamics, difference schemes, stereographic coordinates, vortices.

20. ABSTRACT (Continue on reverse side if necessary and identify by block number)

Three difference methods are developed for calculating the motion of a shallow atmospheric layer on a sphere. The forced motion can be described as the movement of three subtropical highs and a polar low, in each hemisphere. Approximations of such motions were developed from the study of the movement of

20. Abstract - continued

atmospheric vortices (analogous to the classical Helmholtz vortices of potential theory).

It is intended that long period integrations be performed, in order (a) to determine the feasibility of obtaining "accurate climatic forecasts" by numerical methods, and (b) to evaluate the efficiency of the various numerical methods.

A brief summary is given of the work in progress. This is followed by a list of ARPA sponsored CIMS-NYU publications.

5. Type of Report and period covered (cont)

6/1/73 - 5/31/74, 6/1/74 - 1/31/75.

NYU. IMM-407 c.2

Stoker

AUTHOR

Final report, I.

TITLE